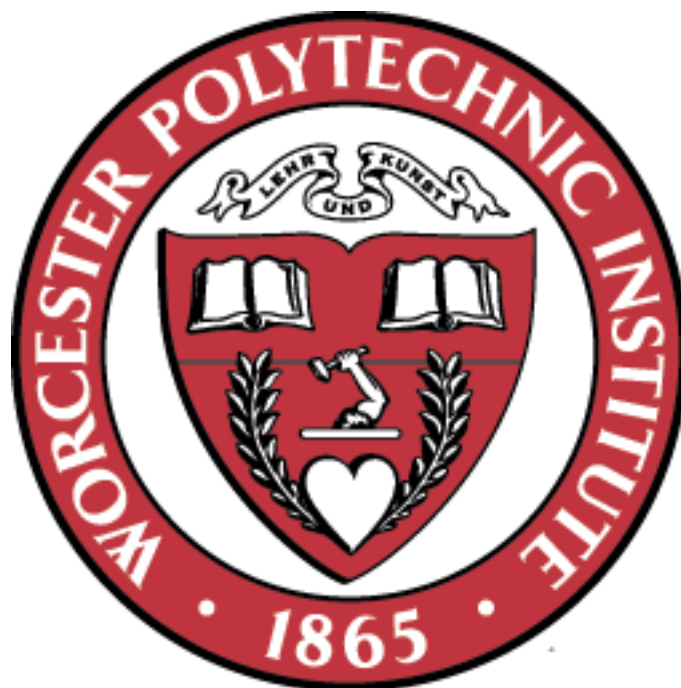# Metal Oxide Photoelectrodes for Water Decontamination

Major Qualifying Project

Chemical Engineering Class of 2019

4/25/2019

Salvador Alvarado

Ryan Choate

Matthew Scanlon

Alan Phung

Abstract

The goal of this project was to develop visible-light activated photoelectrodes using metal oxides to decontaminate water. Some metal oxides used in the production of these photoelectrodes are unstable, so a secondary goal to establish protective outer coatings to be used in tandem with the metal oxides arose. WO_3 and $BiVO_4$ were identified as efficient and effective metal oxides to be used in the development of photoelectrodes, as well as NiO and CoO in the use of the protective coatings.

Acknowledgments

Executive Summary

There is a need for more efficient and more sustainable methods to purify drinking water in circumstances such as disaster relief areas and military personnel use. One method that is currently being used to purify drinking water is solar decontamination using metal oxide photoelectrodes. Most of the research in this area has been focused on TiO_2; however, its effectiveness is very limited due to the high amount of energy required to drive the decontamination reaction. It can drive the reaction using the small percentage of UV light that reaches the earth's surface. The purpose of this project was to determine other metal oxide photoelectrodes that may be activated when exposed to visible light, but also remain stable and not degrade over time.

The reason why TiO_2 is not efficient is due to its large band gap; only UV light, 10% of the light provided from sunlight, has enough energy to overcome the gap and drive the reaction. To achieve a more efficient photoelectrode, metal oxides with smaller band gaps, such as WO_3 and $BiVO_4$, were employed and experimented with. Although the smaller gaps of these materials allow them to drive the reaction under conditions with visible light, a consequence of the increased efficiency is lower stability. One way to counteract the loss of stability within these photoelectrodes is to add a protective outer layer of a different, non-toxic metal oxide. The protective layers that this project focused on were NiO and CoO.

The procedure followed to produce the photoelectrodes started with making a homogeneous precursor solution of the metal oxide. The solution was applied to fluoride-doped tin oxide (FTO) glass using different methods such as spin-coating, spray-coating, dip-coating, and drop-coating, were experimented with throughout the project. Once the solution was added to the FTO glass, it was placed in a box furnace to anneal. The purpose of the annealing process was not only to dry the metal oxide onto the glass, but also to boil off the extra products of the solution to ensure that the only material left on the glass was the metal oxide required. Then, depending on which one was being produced, this procedure would be repeated multiple times for the different metal oxides for which the photoelectrodes were comprised of. Lastly, the photoelectrodes were placed in a cuvette filled with water and an organic dye, exposed to light from a Xenon lamp,

4

and had a voltage applied to them to determine the effect to which they decontaminated the water.
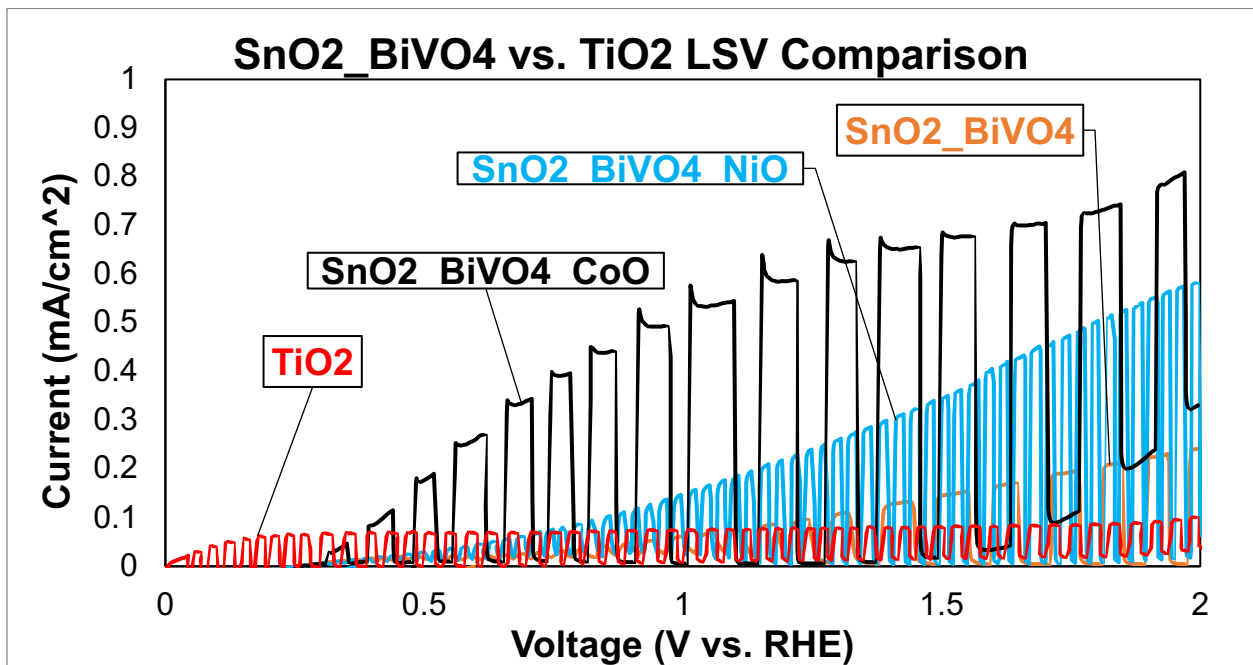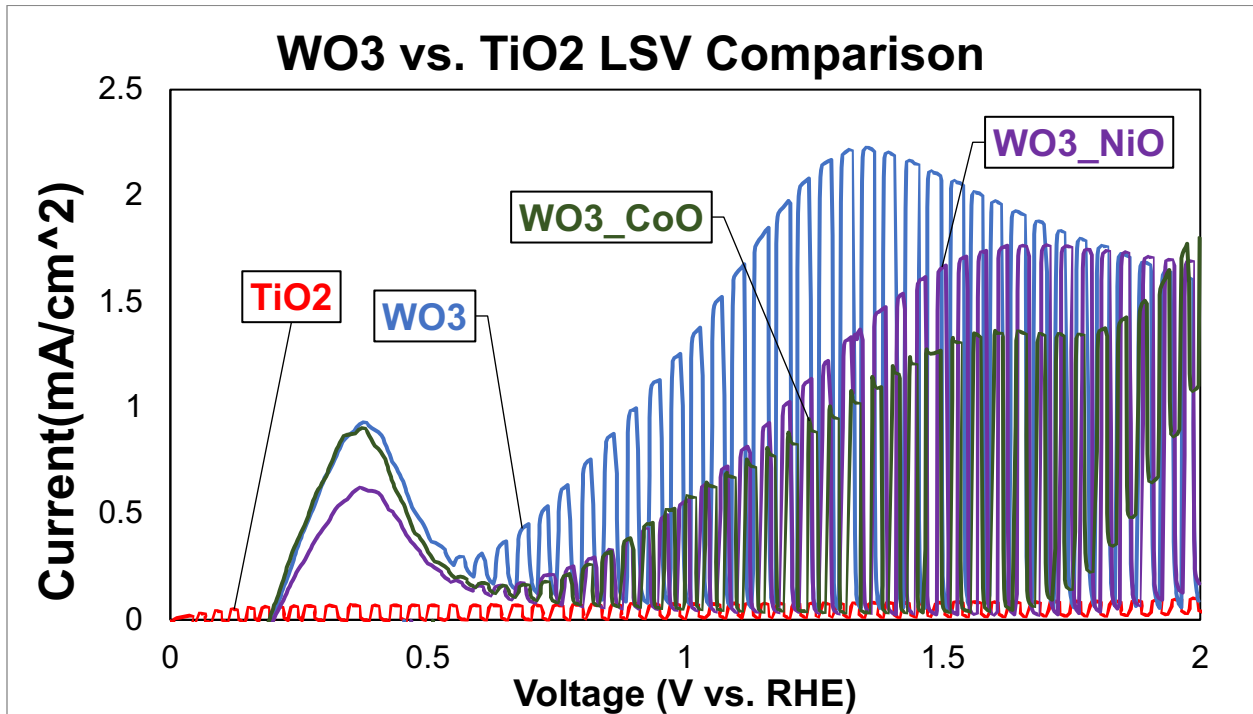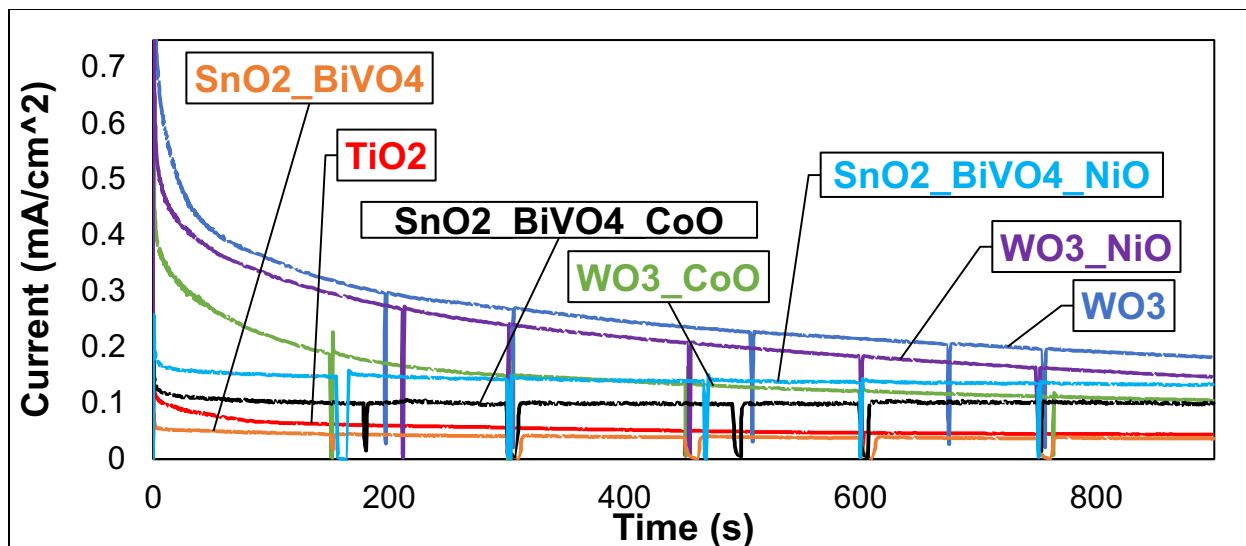
In conclusion, out of all the application methods, spin-coating provided the most consistent and most even layers throughout the experimentation. It was determined that WO_3 and $BiVO_4$ were more effective than TiO_2 at decontaminating the water of the organic dye. Additionally, the NiO and CoO protective coatings proved to promote the stability and longevity of the photoelectrodes. The next steps to take for this research is to increase the efficiency of the WO_3 and the $BiVO_4$ photoelectrodes through the optimization of the electrode to create a larger surface area and different crystal structures. Similarly, a next step is to increase the efficacy of the protective coatings to provide even more stability to the photoelectrode.

Table of Contents

7

Table of Figures

11

1. Introduction

1.1.   Motivation

Soldiers, people in humanitarian crisis, and those in remote areas constantly need to purify drinking water. Though there are methods to accomplish this, such as boiling the water, the source of a fire or stable heat is not always available. Soldiers are even restricted from making fires at times as they may expose their position. Some methods the military and people in humanitarian crisis often use are dissolvable iodide tablets and carbon filters. Though quick and portable, they often struggle with some organic contaminants and their use can be dangerous for many people including those with an iodide allergy or people over the age of 50.[1, 2]

A newer and even more robust method the military uses in disaster relief is solar decontamination (SODIS). It works by using the ultraviolet rays (U.V.) from the sun to kill bacteria and other contaminants[1]. Figure 1 below describes how SODIS is used in the field.
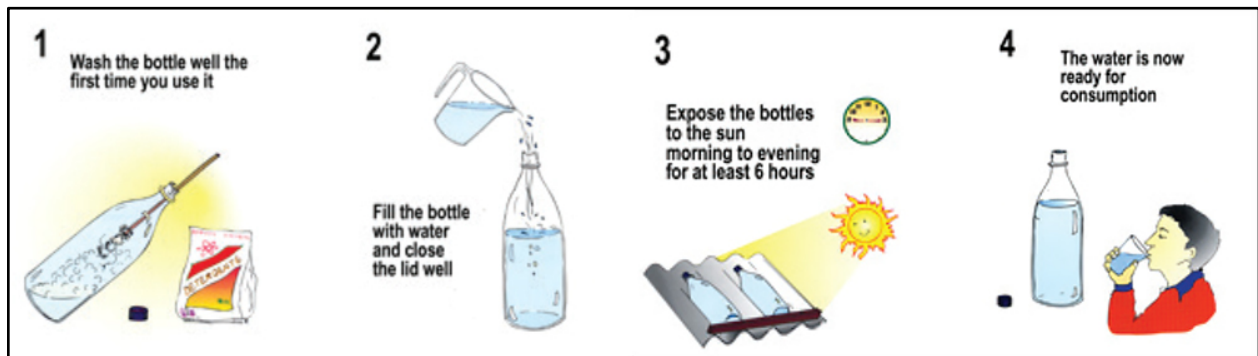
Figure 1: Solar Water Decontamination (SODIS) Used in Military and Humanitarian Relief [3]

Figure 2: Hydroxide & Hydrogen Radical production from U.V Light
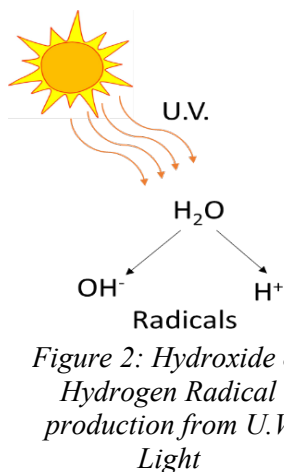
Though it is effective and does not involve the use of potentially hazardous chemicals, this method takes at least 6 hours to work and is extremely dependent on the location, time of day, and available materials. [3]

The main driving force behind the SODIS method is the intense U.V. rays from the sun. They have enough energy to split down chemically stable bonds into unstable radicals within a solution. As a result, these unstable radicals start to bond and break down other stable compounds. These stable compounds include many organic contaminants found

within water and typically break down to very basic components such as more water and carbon dioxide. [4]

Many recent studies have found that a similar method to SODIS may be quicker and even more effective. It involves the use of a photoelectrode to help activate and split water into radicals with even less energy than that of the U.V. rays.

1.2.   Overview of Project

The focus of most research in this field has been on titanium dioxide as it was the first material discovered that was able to cause this degradation. TiO_2 produces hydroxyl and superoxide radicals when exposed to UV light which react with organic compounds reducing and oxidizing them to simpler compounds like water, carbon dioxide, and oxygen gas.

Although TiO_2 is effective in producing these radicals, its effectiveness is hindered because it is only activated by 10% of the wavelengths of light that reach the surface of the earth.[5]

Other metal oxide photoelectrodes that produce the radicals when exposed to wavelengths of visible light have been explored as alternatives to TiO_2.[6] Visible light activated photoelectrodes allow for a wider range of light wavelengths to be utilized as well as a larger percentage of the total solar energy.

Figure 3: Hydroxyl radical and super oxide production from photoelectrode in water under light

The purpose of this research is to identify and produce efficient, stable, and non-toxic visible light activated metal oxide photoelectrodes that can be used in the purification of drinking water.

14

2. Background

2.1.   Water Decontamination

Water decontamination is defined by the EPA as "the inactivation or reduction of contaminants from surfaces by physical, chemical, or other methods to meet a cleanup goal." With today's growing population and scarcity of clean drinking water, a large amount of research has been dedicated to finding cheap, efficient, and practical water decontamination methods.[7, 8]

Some popular decontamination methods have been focused around adding a variety of chemicals to the water to eliminate contaminants. These methods are "chemically, energetically and operationally intensive, focused on large systems, and thus require considerable infusion of capital, engineering expertise and infrastructure, all of which precludes their use in much of the world." For many people living in less developed areas, these methods are infeasible. For others who may have access to these decontamination methods, oftentimes will suffer from their negative effects.

In recent years, a significant amount of research has been dedicated to the decontamination of water without the addition of chemicals. Advanced oxidation processes (AOPs) focus on water decontamination using radicals within a solution to break down contaminants. The most common example of this system is the production of hydroxyl and superoxide radicals from water. When these radicals are produced, they encounter contaminants and oxidize them forming CO_2, other inorganic ions, and organic minerals. These radicals are extremely reactive and will break down most organic contaminants, as well as kill small microbes, making them extremely effective at decontamination.[9]

In addition to their high reactivity, AOPs are also advantageous as they can be produced using several methods. The simplest form this takes is the SODIS method mentioned before, where water is left in a closed container exposed to UV lights for multiple hours. UV light dissociates water molecules within a solution into superoxide ($O_2\bullet$) and hydroxyl ($\bullet OH$). Once a radical molecule is made, it interacts with other molecules perpetuating the reaction. This method requires a lot of time and because it is directly dependent on UV light, it ends up being inefficient because not much UV lights passes through the atmosphere, and requires direct exposure to sunlight, which is very dependent on geographic location.

A less energy intensive method for producing AOPs is using photoelectrodes. Photoelectrodes act as semiconductor catalysts by speeding up the reaction for the radical production on their surfaces. The use of photoelectrodes to decontaminate water is described in the Photoelectrodes section.

2.2.   Semiconductors

Semiconductors by their nature are neither perfect insulators nor conductors. They work by having electrons in the valence shells of the material be excited by some form of outside energy (e.g. heat, photo-energy, mechanical) up to a higher energy level where it can then conduct electricity. The energy level of these valence electrons is the valence band and the energy where the material conducts electricity is the conduction band. The amount of energy between these bands is called the band gap and refers to the amount of energy needed to excite the valence electrons up to the conductive state.[10]

When multiple materials are involved in a semiconductor, there are two types in reference to these electrical potentials called n-type and p-type. N-type materials have many excitable electrons and p-type materials have positive orbital holes which can be filled by excited electrons. It is possible to combine or layer n-type and p-type materials in order to optimize electron transfer.

2.3.   TiO$_2$ Current Technology

TiO$_2$ has long been used as an important component in many industrial products. It was originally used in paint mixtures to increase the paint's whiteness and opacity. More recently, research has found it to be extremely good at absorbing U.V. waves emitted from the sun. Due to this ability, it began to be adopted into the skin-care industry for U.V. protection in sunblock and moisturizers. [11]

TiO$_2$'s latest application has been in the photoelectric field. As it can absorb U.V. radiation, this gives it a unique ability to produce, as some sources say, "self-cleaning" surface capabilities due to the radical production described following section section.[11].

2.4.　　Photoelectrodes

Photoelectrodes found in this experimental system are solar cells that directly interface a semiconductor with an electrolyte to produce •OH through a process akin to electrolysis of water. Instead of decomposing water into hydrogen and oxygen gas, the process decomposes water into •OH and O_2•. Unlike with normal water splitting, they do not require a separated membrane like in an electrolyzer, and as a result reduce system complexity and potential loss channels. They are comprised of two photosensitive semiconductor plates (an anode and cathode), connected by wire to promote the flow of electrons. When placed in water and exposed to sunlight along with an applied voltage, the decomposition of water occurs, and production of hydroxyl and superoxide radicals begins. Photoelectrodes are invaluable within the context of water decontamination.[12] [13] [14]

Using Advanced Oxidation Processes (AOPs), they can purify water containing organic compounds. This is achieved through the production of hydroxyl radicals, which oxidize and mineralize a significant majority of organic material. Therefore, they have wide applications and uses due to the simplicity and robustness of the individual cells. They can be manufactured as personal water purification systems for nature enthusiasts or distributed in mass to soldiers and service men/women. They may also be scaled up to provide large scale water purification for communities and groups of families.

Photoelectrodes work by having light energy excite electrons in the valence band to the conduction band energy level. TiO_2, for example, has a band gap that stretches 3.2 electron volts (eV); this relatively large band gap is the reason why TiO_2 is only able to produce the radicals using high energy UV light.

The hydroxide radical reaction requires a voltage gap of 2.38eV which is the difference between its energy level and the hydrogen evolution reaction ($2H^+ \rightarrow H_2$) which we are defining at 0eV. This voltage gap corresponds to the activation energy of the reaction. TiO_2 falls well within this energy gap, and even reaches into the superoxide reaction range (-0.33eV relative to the hydrogen evolution reaction).[15] However, the efficiency and rate of treatment of water using TiO2 and ordinary sunlight is severely limited by this large band gap and can only utilize a small portion (~3.8%) of the power of sunlight that is in the UV range. [5]

17

Bi₂WO₆   TiO₂

-0.33eV (O2/O2•)

0eV (H+/H2)

3.2eV

2.7eV

1.23eV (H2O/O2)

2.38eV (H2O/O2•)
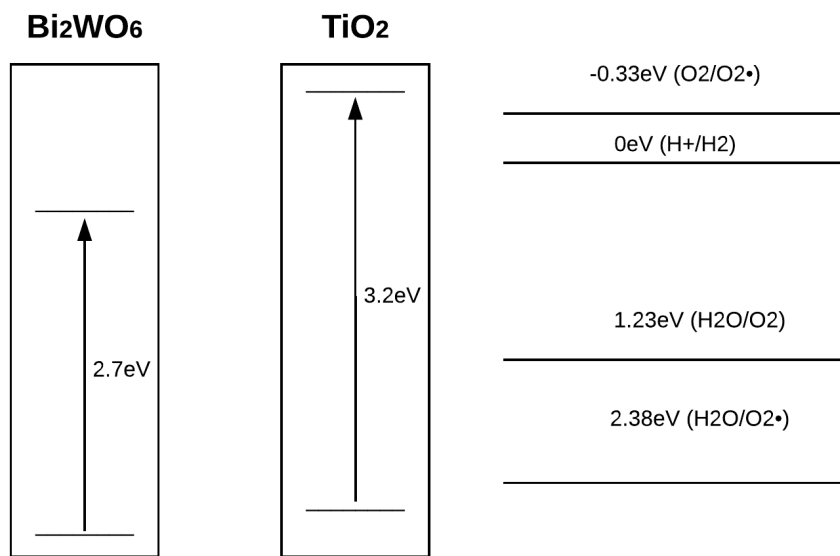
Figure 4: Electron energy intervals of TiO2 and Bi2WO6 relative to hydrogen evolution reaction

A material with a smaller band gap would be able to absorb light in the visible light range and still produce the hydroxide radicals. The cost of having this smaller band gap is that superoxide radicals cannot be produced by the same material; however, this can be solved by using a photocathode in tandem.

2.5.   Visible-Light Activated Photoelectrodes

Metal oxides like bismuth tungstate, tungsten oxide, bismuth vanadate, etc. have a sufficiently sized band gap to absorb visible-light and produce hydroxyl radicals and superoxides. For certain cells such as $BiVO_4$, hydrogen peroxide is produced in place of the hydroxyl radicals and superoxide.[16] A sufficiently sized band gap does not necessarily mean that these other metal oxides are more photo-catalytically active than TiO_2, but past studies show comparable or improved activity.[17]

Often the issue that arises with these metal oxides is that they are not as chemically stable as TiO_2. This means that the electrodes themselves degrade over time and lose the ability to produce the hydroxyl radicals. Furthermore, although materials like TiO_2 (in this structure) are non-toxic, if an unstable material like cadmium oxide were used, it could itself contaminate the water.

2.6. Photoelectrode Protective Layer

A possible solution to these issues is to use a metal oxide that is more photo-catalytically active than TiO_2 and then cover it with a thin layer of a non-toxic metal oxide. If developed, it would create highly effective photoelectrodes that could be applied in purification of drinking water due to the non-toxicity.

Though practical in application, finding a coating that is strong and compatible with the photoelectrode presents challenges within itself. According to *Hu et al* , the protective film layer should possess certain properties such as being thermodynamically stable and having a large barrier for transfer of the majority carriers of the base photoelectrode.[18] Most of the metal oxides that are being tested for this project are n-type semiconductors; consequently, it would be ideal to use a p-type semiconductor material as the protective layer. One of the desired properties for the protective layer is to have a large transfer barrier for the base electrode's main carriers (electrons). This transfer barrier is caused by using a coating material with a conduction band above the conduction band, and therefore closer to vacuum, of the base electrode material.

2.7. Linear Sweep Voltametry (LSV)

Linear Sweep Voltametry is used to study the electron transfer kinetics and the transport properties of the electrolysis reactions within the cell[19]. A fixed potential range was set and used to find the current response by sweeping from one point to the other. By comparing the LSV responses of each cell, the amount of current produced under the applied voltage range can be directly compared.

Within the experimental system used in this study, two LSVs were conducted per cell. One with a solar xenon lamp turned on and aimed at the cell, and one with the lamp turned off. This allowed us to see the difference in produced current from each cell. The hope is that, with the light turned on, there would be a high amount of current with a lower applied voltage. This would mean the photovoltaic cell is properly working and activated by the use of the lamp.

2.8.   Chrono-Amperometry (CA)

Chrono-amperometry is defined as" An electrochemical technique where the time dependence of the cell current is measured whilst the potential difference between the indicator and reference electrodes is controlled."[20] Within the experimental system, it is used to see the degradation of the cell over time while it is in use. The xenon lamp is aimed at the cell while testing the amount of current produced by the cell over time. As time passes, the decrease in current is measured and graphed. The hope for the produced cells is to have the least amount of current-loss over time.

2.9.   Dye Degradation

Dye degradation within the system is used to study the break-down of an organic dye from the production of hydroxide and superoxide radicals from the photoelectrode cell. The dye in this case, is used to model some of the most common water contaminants found in different sources of water. A basic schematic of this concept can be seen in figure 5 below:
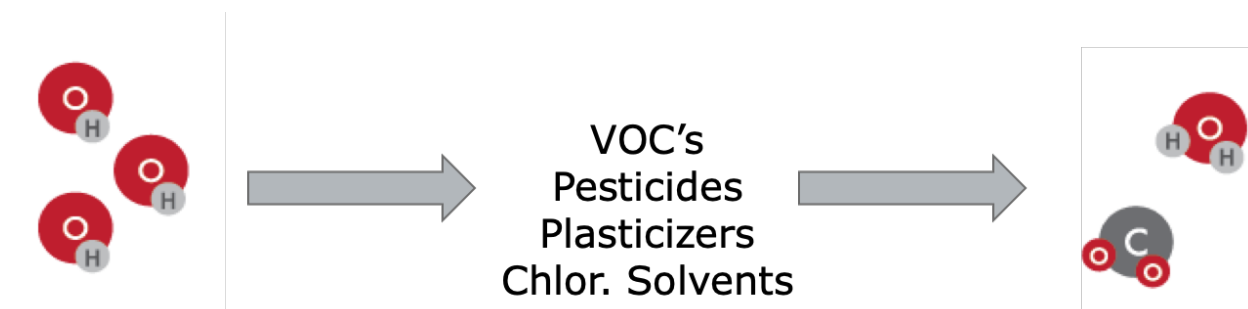
Figure 5: Organic Contaminant Decontamination Using Photoelectrolysis Products. Oxidation of organic contaminants

Using a dye also allows for optical estimation of concentration following the Beer-Lambert law. The dye is degraded into smaller compounds like oxygen, water, and smaller organic acids.[21]

3. Experimentation

3.1.   Dye Selection

Much of the research surrounding photocatalytic degradation has used the methylene blue dye to track degradation over time. The issue with methylene blue is that the absorption spectrum has multiple peaks within the visible-light wavelengths, making it difficult to calculate the concentration. [22]
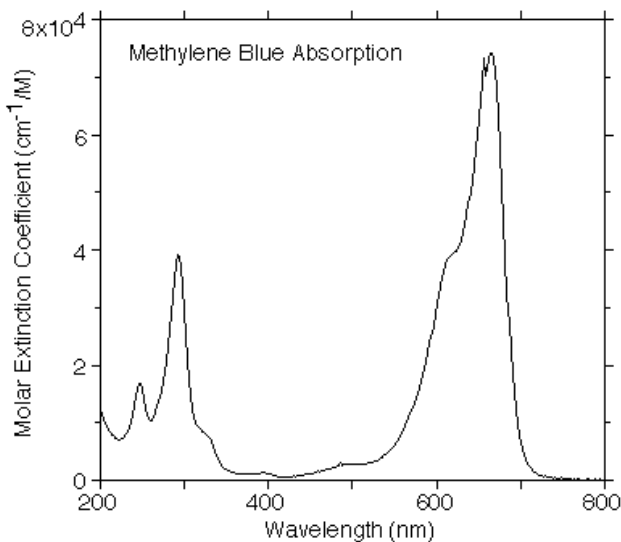
Figure 6: Methylene Blue Absorption Spectra Showing Double Peaks in the Defined Range [23]

Other dyes like methyl red and methyl orange have also been used in studying the effectiveness of photoelectrodes. These dyes are advantageous because they only have one distinct absorption peak in the visible light spectrum. Having only one peak allows you to discern if the absorption spectrum measured is due to a secondary product after initial degradation of the dye compound. Other dyes like methyl red and methyl orange have also been used in studying the effectiveness of photoelectrodes.[24]
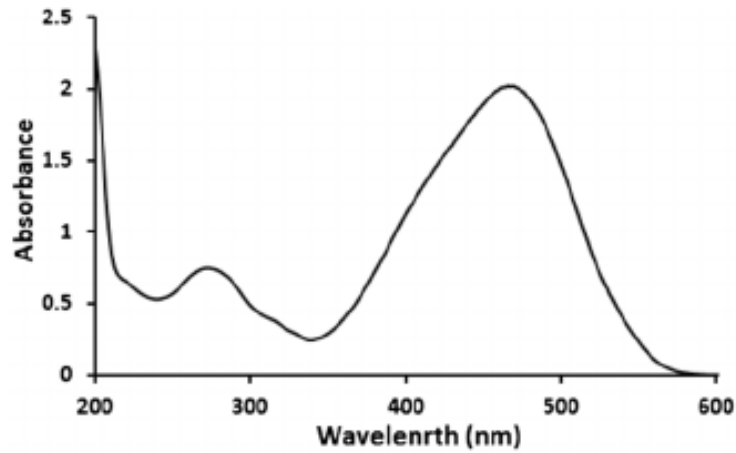
Figure 7: Methyl Orange Absorption Spectra Showing Single Peak in Desired Range [25]

Methyl orange has also been found to be stable in visible and UV light (250nm-800nm) whereas methylene blue degrades when exposed to light of these wavelengths. Using a dye like methyl orange enables the conclusion that the degradation is due to the photoelectrode's produced radicals, and not any other factor such as the light itself..[26] In all the dye degradation tests, a solution of methyl orange was used as the organic dye.

3.2.   Preparation of the Electrodes

Seven types of electrodes were synthesized: a TiO$_2$ electrode, a WO3 electrode, two WO3 electrodes with NiO and CoO coatings respectively, a BiVO4 electrode, and two BiVO4 electrodes with NiO and CoO protective coatings respectively. All of the electrodes were made on a 4.5cm x 1cm piece of fluorine-doped tin oxide (FTO) coated glass. Tape was placed covering 1cm^2 of the glass and then as removed after the spin-coating, or after the first layer was placed in the case of BiVO4. The metal oxide solutions were prepared using the following methods.

3.2.1.   Titanium dioxide (TiO$_2$)

Diluted TiO2 paste in ethanol at a ratio of 100% w/w in a glass vial. The mixture was sonicated for 2 hours until the paste was completely dissolved. Drop-casted 200µL of the solution onto the FTO glass and spin coated the glass at 3000rpm for 15s. Annealed the electrode in a box furnace at 500°C for 1 hour. This produces a TiO2 layer approximately 1 micron thick.

3.2.2.   Bismuth tungstate (Bi2WO6)

55mM bismuth meta-tungstate hydrate (Bi(NO$_3$)$_3$·5 H$_2$O) and 27.5mM (NH$_4$)H$_5$[H$_2$(WO$_4$)$_6$]·H$_2$O were individually dissolved in 5 mL of ethylene glycol. These solutions were mixed in a volume ration of 1:1, and a white transparent precursor solution was obtained after ultrasonication for 1h. Drop-casted 0.2 mL of the mixed solution onto 1.5cm x 1cm FTO by pipette and annealed in a furnace ramping from 20C to 500C for 4 hours to achieve 2C/min.

3.2.3.   Tungsten trioxide (WO$_3$)

Added 1.6g of ammonium metatungstate hydrate (AMT) and 0.6g of 6000 chain length polyethylene glycol (PEG) per mL of water to a vial and then sonicated it until dissolved. The PEG acts as a thickening agent to increase the viscosity of the mixture for the spin-coating. 300µL of the mixture was then dropped onto the FTO glass and spin-coated at 3000rpm for 15s. They were then placed in a box furnace ramping up to 550°C for 2 hours and then holding at 550°C for 2 hours.

3.2.4. Tin oxide/Bismuth vanadate (SnO$_2$/BiVO$_4$)

First a tin oxide (SnO$_2$) layer was made by dissolving 0.49g of SnCl$_2$ into 10mL 2-methoxyethanol and sonicated the mixture overnight. 100μL of the solution was then dropped onto the FTO glass and spin-coated at 2000rpm for 40 seconds. The coated glass was then placed on a hotplate at 500°C for 10 minutes. After allowing the glass to cool, 100μL of the solution was added again and spin-coated. This process was repeated until 4 layers were added, and then the glass was placed into a preheated box furnace at 550°C for 2 hours.

For the bismuth vanadate (BiVO$_4$), first 0.1225g of bismuth nitrate Bi(NO$_3$)$_3$ was added to a vial with 5mL of acetic acid (AA) and sonicated for 10 minutes. After the Bi(NO$_3$)$_3$ dissolved, 0.0633g of vanadyl acetyl acetonate (VAA) was added as well as 0.25mL of acetylacetone (AO) and then sonicated for ~20minutes. 11.6μL (5μL per cm^2 of glass) of the solution was then dropped onto the SnO$_2$ layer and then heated at 500°C on a hot plate for 10 minutes. After allowing the glass to cool, this process was repeated until 6 coatings of the solution were added. The glass was then placed in a box furnace ramping to 450°C for 30 minutes and holding at 450°C for 1.5 hours.

3.2.5. Nickel oxide (NiO)

Nickel oxide (NiO) was identified to be a suitable p-type coating for the photoelectrode cells. A solution of 0.05M nickel chloride (NiCl$_2$) was prepared to coat the cells. When exposed to heat and air, the Cl$_2$ oxidizes, leaving behind NiO. After preparing the photo-electrode cells, four methods were used to coat them with the nickel oxide. The first method was drop coating the cells. A 1000 μL automatic pipette was used to drop 300 μL of nickel chloride onto the prepared cells. The cell was then heated to 350 C and left for 30 min.

The second method involved the same procedure, dropping 300 μL of nickel chloride onto the cell and spinning the glass with the nickel chloride solution. Each cell coated this way was placed in the spin coater and ran at 500 rpm for 10s. The cells were placed in a box furnace that ramped to a set point temperature of 350 C at 10 C / min. Once the samples dried, the NiO coating may be observed over the cells.

24

Additionally, a technique using spray-coating was used to coat the cells. In this method, glass was heated to 350 C on a hot plate. Once heated, a solution of 0.05 M Nickel Chloride was sprayed onto the top at a rate of 2 mL/min for 5 min. The results for this method can be seen in section 1.1.8.[27]

The final method that proved to work the best for producing nickel oxide was another spin-coating procedure. To produce the nickel oxide, nickel nitrate hexahydrate and nickel acetate tetrahydrate were added together in a 9:1 molar ratio of nitrate to acetate. Then methanol was added to the above mixture and was sonicated until everything was completely dissolved. For this project, 0.785 g of nickel nitrate hexahydrate and 0.075 g of nickel acetate tetrahydrate was dissolved in 3 mL of methanol. Then triethanolamine (TEA) was added using 0.5:1 molar ratio of TEA to nickel. After adding TEA, the solution was sonicated until it was completely mixed. For this project, 0.2 mL of TEA was added to the mixture. After completely mixing, 300 microliters of the solution were spin-coated on the FTO glass at 3000 RPM for 50 seconds. Lastly, the cells were annealed ramping up to 550 degrees C for 2 hours and then at a constant temperature of 550 degrees C for 2 hours.

3.2.6.   Cobalt oxide (CoO)

Cobalt oxide (CoO) was also identified to be a suitable p-type coating for the photoelectrode cells. To produce the cobalt oxide, cobalt nitrate hexahydrate and cobalt acetate tetrahydrate were added together in a 9:1 molar ratio of nitrate to acetate. Then methanol was added to the above mixture and was sonicated until everything was completely dissolved. For this project, 0.786 g of cobalt nitrate hexahydrate and 0.075 g of cobalt acetate tetrahydrate was dissolved in 3 mL of methanol. Then TEA was added using 0.5:1 molar ratio of TEA to cobalt. After adding TEA, the solution was sonicated until it was completely mixed. For this project, 0.2 mL of TEA was added to the mixture. After completely mixing, 300 microliters of the solution were spin-coated on the FTO glass at 3000 RPM for 50 seconds. Lastly, the cells were annealed ramping up to 550 degrees C for 2 hours and then at a constant temperature of 550 degrees C for 2 hours.

The following shows an exploded diagram of the final cell layers:

Protective Oxide
Absorbing Oxide
Mesoporous Tin Oxide
Fluoride Doped Tin Oxide (FTO)
Glass
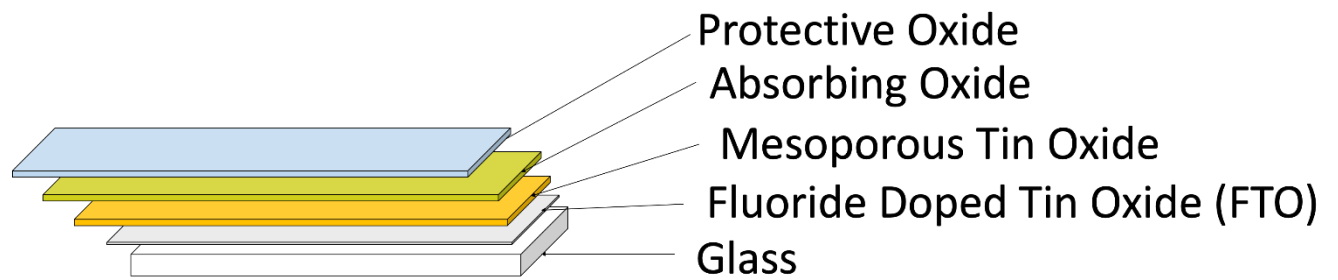
Figure 8: Exploded diagram showing each layer of the photoelectrode cell

3.3.   Metal-Oxide Application to Glass & Other Layers

Different methods were studied and tested to best adhere layers to the base glass as well as previously coated layers. The methods that were used are described below:

3.3.1.   Drop-Coating

Drop-coating was tested as it is a common technique used in photoelectrode coatings [28]. This technique starts with the preparation of the coating, then to dropping a small amount onto the surface (usually enough to cover it completely), and lastly annealing the cell. The annealing stage would oxidize any material and evaporate any unwanted solvents from the solution such as water. This method was used during earlier trials; however, it was problematic due to the uneven spreading of material. Additionally, it left a lot of random patches of uneven residue visual on the surface that refracted light hitting the surface. This was a easily reproducible method to use, and did not add any complexity to the overall process of making the electrodes.
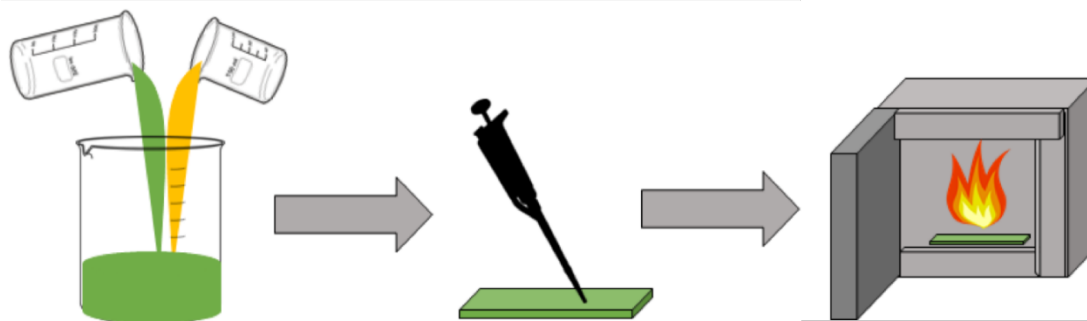
Figure 9: Drop-Coating procedure used for early cell coatings

3.3.2.   Dip-Coating

Dip-coating is another common technique used in photoelectrode coatings. It is commonly used when thin layer coatings such as the ones that were being synthesized in this procedure are desired. In drop-coating, the layer thickness is directly proportional to the speed in which the cell is removed from the base liquid. The faster the speed, the thinner the layer and vice-versa[29]. The dipping stage of the process can be seen in the image below:
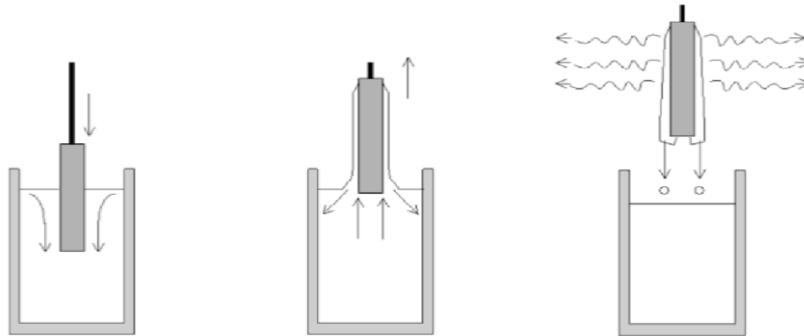
Figure 10: Dipping-step of dip-coatings for photoelectrodes [29]

Dip coatings are known to be difficult to control without the use of advanced equipment. Even though this is true, a robust method, such as using your hand to dip the electrodes can also be used at the sacrifice of precision. Dip coating often leads to the un-even distribution of material as well as when pulling the cell out of the solution, it all flows to one side of the cell. The procedure used for preparation of cells using dip coating can be seen in the figure below:
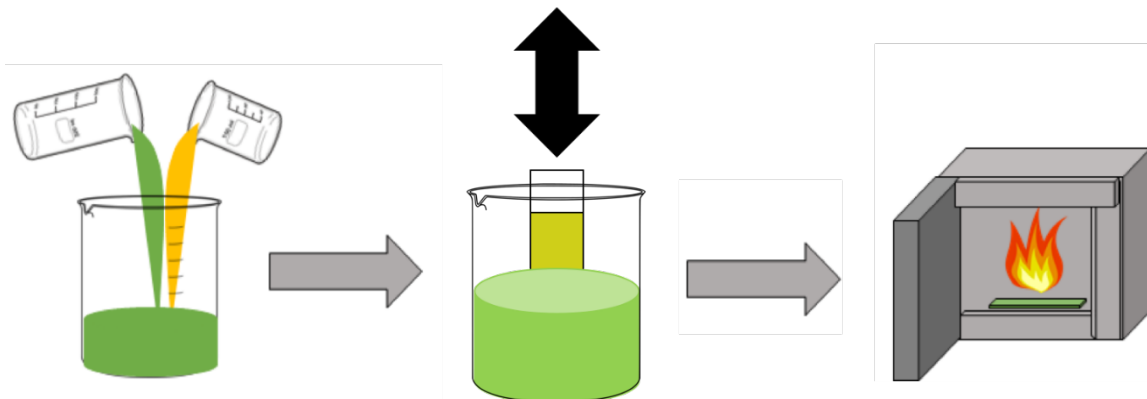
Figure 11: Dip-Coating procedure outline showing the preparation of material, the dipping of the cell, and annealing stage.

3.3.3.   Spray-Coating

Spray-coating is known for its ability to evenly distribute material across a flat surface. In this experimental design, a mister was used to spray material onto the base layer of the cell then anneal it in a box-furnace. This was utilized as it is a fast and relatively simple way to apply these coatings. For this test to be standardized, the amount of volume sprayed by one trigger of the mister was calculated for the mister available in the lab. After which, a specific volume was sprayed onto each cell. The procedure can be clearly seen in the figure below [27].
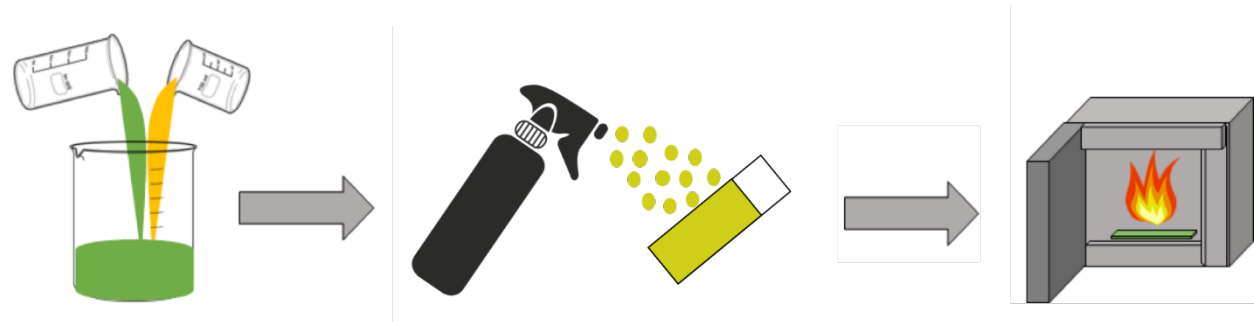
Figure 12: Spray-Coating procedure outline showing the preparation of material, the spraying of the cell, and annealing stage.

3.3.4. Spin-Coating

Spin-coating is one of the most commonly used methods to thinly coat cells. It is similar to drop coating; it starts off with preparing a solution, then dropping it onto the cell, spinning it at a certain rotational velocity (rpm), and lastly annealing. This method too is very simple and gives more process control. The layer thickness can be adjusted by controlling the spin speed during the spinning step of the process. Additionally, this can also be controlled by how much material is added during the dropping section of the procedure. This step is also dependent on the viscosity of the dropped liquid. The spinning is an added benefit to the process as it also ensures the material is evenly spread out onto the surface of the cell prior to the annealing step of the process [30]. The procedure for spin-coating is outlined by the figure below:
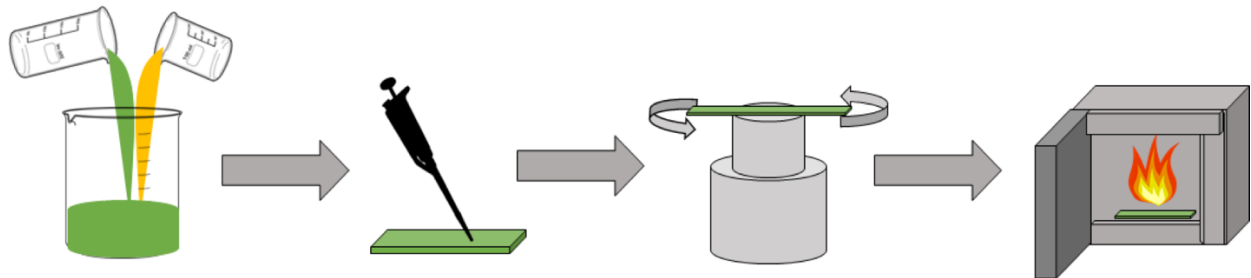
Figure 13: spin coating procedure outline showing the preparation of material, drop-coating, spin coating, and annealing stages

3.4. Testing the Electrodes

3.4.1. Current Efficiency

The electrodes were each put into a beaker with a 40mL solution of DI water with a PH7 buffer solution, a platinum wire counter-electrode, and a SCE reference-electrode. The PH7 buffer was prepared by mixing 150mL of DI water with 10g of potassium dibasic and 4g monobasic and verified using a PH probe. The beaker was placed 13cm away from the aperture of a xenon-solar lamp and 11cm above the surface of the table. The electrodes were tested with the lamp on and off using LSV from -0.657V to 1.343V relative to SCE, which corresponds to 0V to 2V vs. RHE. The LSV test was used to show the efficiency of the electrodes in terms of how much current was induced at the various voltages. A higher current at a lower voltage means that the electrode is more efficient.
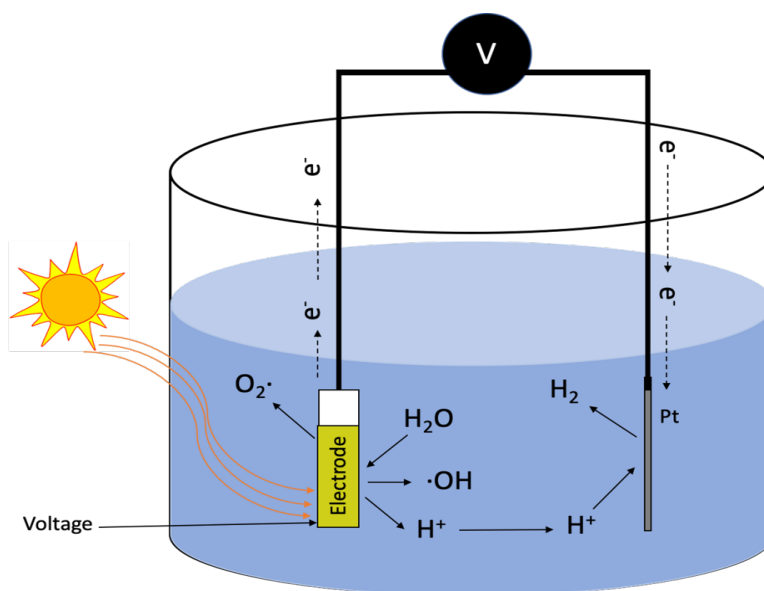
Figure 14: Experimental system showing the Hydroxyl and Super Oxide production when photoelectrode cell is in the presence of sunlight and an applied voltage for the LSV and CA studies.

3.4.2.   Electrode Stability

The stability of the electrodes was tested using chronoamperometry (CA), where a voltage is held constant and the induced current vs. time is observed, at 0.343V vs. SCE which corresponds to 1V vs. RHE. A 50mL beaker was filled with 40mL of the PH7 electrolyte solution and placed with the front of the beaker 13cm away from the aperture of the light machine and 11cm above the surface of the table. The CA test was used to show the stability of the electrodes where the more constant the induced current was over time, the more stable the electrode was.

3.4.3.   Beaker Degradation Method

A beaker was placed 13cm away from the aperture of a xenon-solar lamp. The electrodes were put into this beaker along with 19mL of DI water with a 7PH electrolyte buffer, a platinum counter-electrode, and a SCE reference-electrode. A spectrometer was placed behind the beaker with the solution to measure light irradiance vs. wavelength. Following the Beer-Lambert law, the light absorbance of a solution is directly proportional to the concentration of compound in that solution; therefore, once a dye is completely colorless, the spectrometer reading should be the same value as when there is just water in the beaker. A reading of the light intensity with just DI water and buffer solution in the beaker was taken and then 1mL of 0.2mM methylene blue was added to the solution to make a 20mL solution of 0.01mM methylene blue. 1.3V relative to the SCE was applied to the system for 1hr and readings of the irradiance from the spectrometer were taken every 5 minutes. The same procedure was followed using methyl orange as the organic dye.[31] The following schematic shows how the dye degradation is set-up within the lab.
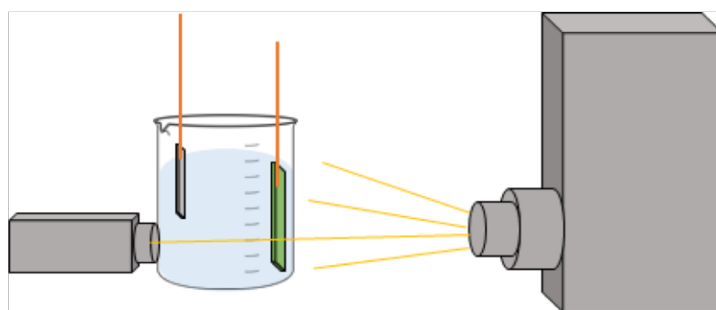
Figure 15: Basic Schematic for Dye Degradation Test showing xenon lamp with direction of light, spectrometer, beaker, water, photoelectrode, and reference electrode

3.4.4.   Cuvette Degradation Method

A 3mL glass cuvette was filled with 2.8mL of the PH7 electrolyte solution and then a cuvette-sized stirring bar was placed at the bottom. The cuvette was then placed into the 3D printed cuvette holder 13cm away from the aperture of the light machine and 11cm from the surface of the table. The spectrometer was then placed in the cuvette holder and the apparatus was secured with tape. After taking a reading of the spectrometer for the clear solution, the electrode was placed into the cuvette as well as the platinum wire counter-electrode and 0.2mL of the concentrated methyl orange solution was added to create a 0.02mM solution if the methyl orange dye. 2V was applied to the system for 1hr using the counter-electrode as the reference electrode. At the end of the hour the electrode and platinum wire were removed and another spectrometer reading was taken to calculate the extent of dye degradation.

The cuvette was used to address the issues of a large volume and curved glass edges scattering light when using the Beaker Degradation Method in Section 3.5.3. The flat edges and small volume of the cuvette solved this. This cuvette had to be fixed in front of the spectrometer to ensure it would stay still during testing and keep the spectrometer readings standardized. A cuvette holder was designed and 3-D printed to ensure the photoelectrodes, wires, and clips could be attached to and from the experimental system without moving the cuvette away from the spectrometer.
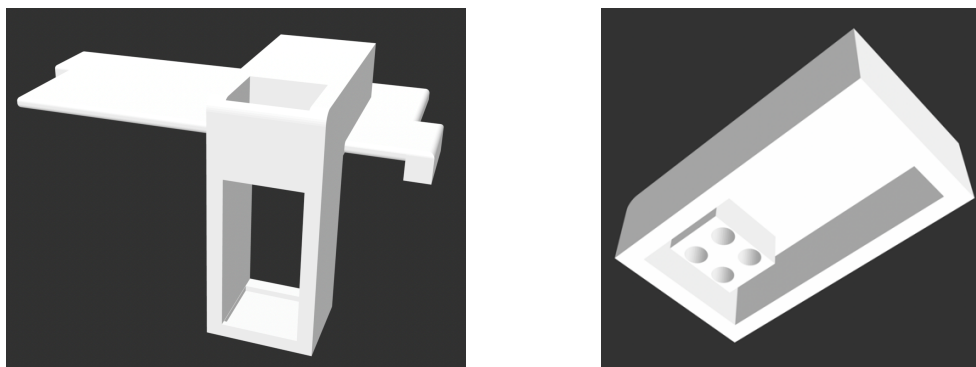
Figure 16: (Left) Body of the Cuvette Holder showing the top opening for the cuvette and side opening where light from the xenon light shines through. (Right) Cuvette Holder Cap that fits atop the top hole and secures the cuvette to the holder

A photo of the experimental setup using the cuvette holder in use can be seen in the following image:
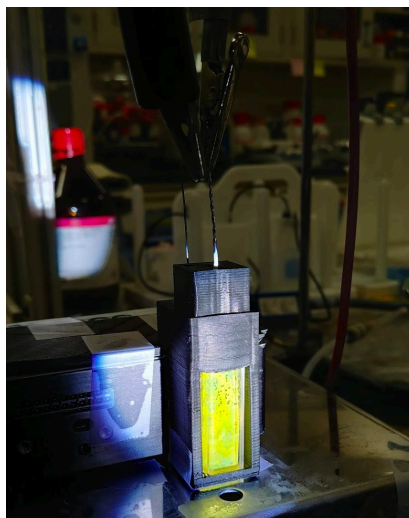
Figure 17: Cuvette Holder in use atop the spectrometer. Green WO3 Cell in the line of the opening leading to the cuvette with Methyl Orange Dye, leading to the spectrometer opening. Wires connected to the photoelectrode and reference Pt electrode.

4. Results

4.1.   Dye Efficacy

The dye used to model organic contaminants was tested to see its effectiveness in the experimental system. The results are outlined in the following sections.

4.1.1.   Methylene Blue

Tests run using the Beaker Dye Degradation procedure defined in Section 3.5.2. TiO_2 and bismuth tungstate (Bi_2WO_6), as well as Bi_2WO_6 coated electrodes, were tested to find which degraded methylene blue dye most efficiently. The molarity of the solutions over time using the different electrodes (and the dye without photoelectrode assistance) were calculated by comparing the ratio of the difference in magnitude of the spectrometer reading at 660.91nm (as this is close to the absorption peak of methylene blue) to the when the dye was originally added and the clear PH7 solution every 5 minutes up to one hour starting when the dye is added.
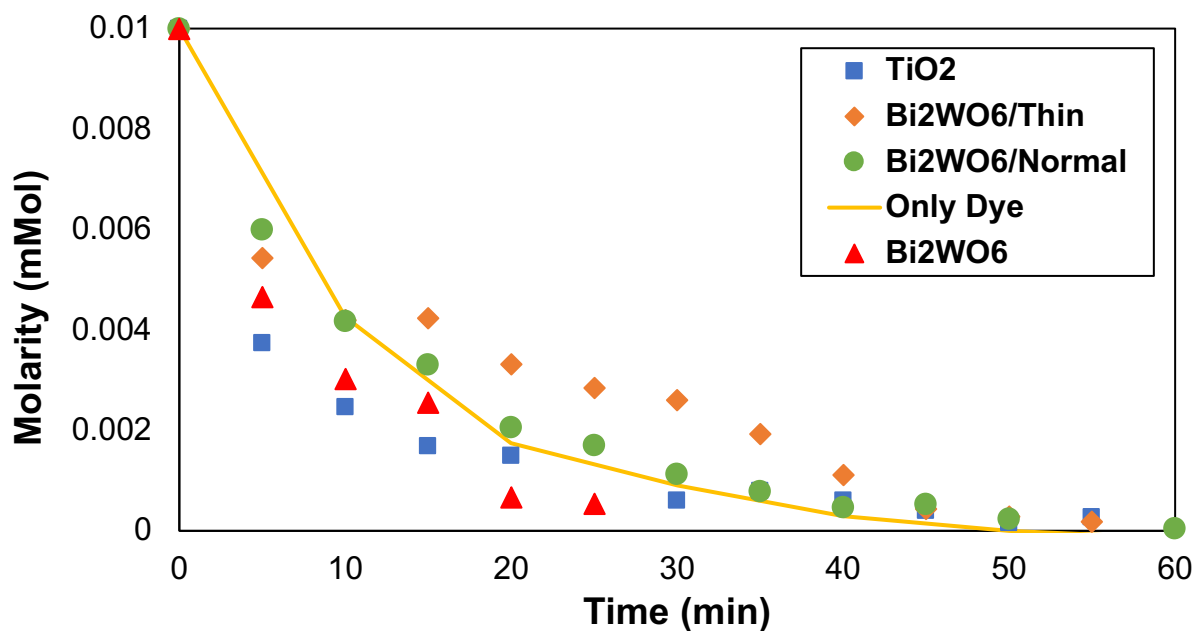
Figure 18: Comparison of degradation of methylene blue using different electrodes in 20mL of mM methylene blue in water with PH7 buffer and 1.3V vs. an SCE reference electrode and a control of 20mL of mM methylene blue in water with PH7 buffer exposed to the light.

As can be seen, methylene blue degrades just by exposure to light without any photoelectrode assisted radical production. It was also confirmed that it degrades not just be exposure to UV light, but also to solely visible light by running the same test with a UV filter over the solar machine. The data for this can be seen in Appendix A. Although methylene blue was chosen because many papers reference it as a suitable dye to test degradation, it was found unviable, as it would become unnecessarily difficult to calculate what amount of degradation was due directly to light exposure and what was because of the radical production.
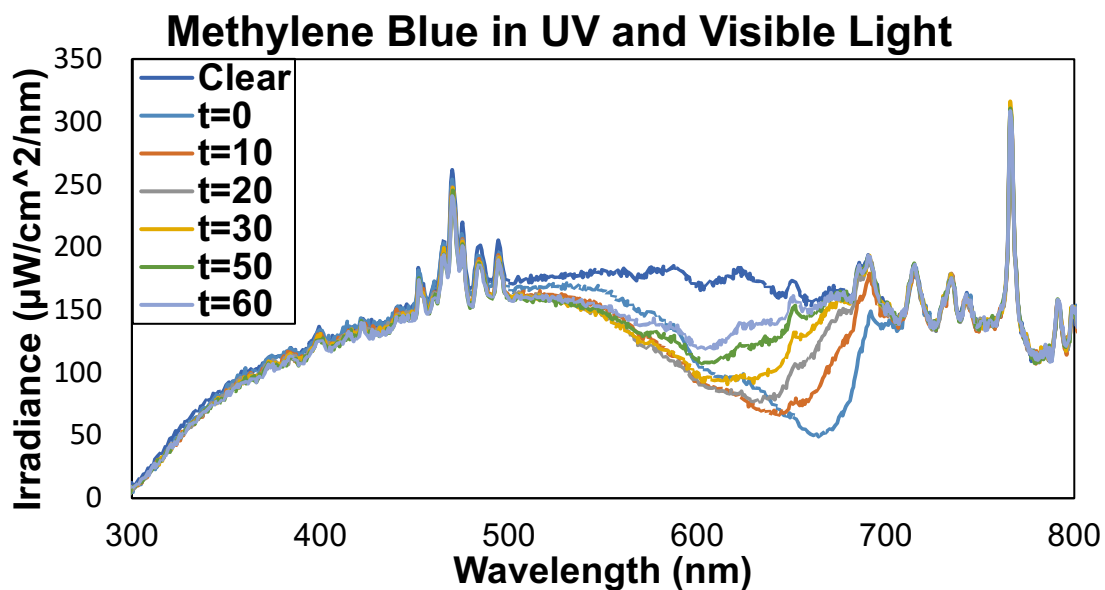
Figure 19: Spectrometer reading of absolute irradiance through the solution from the addition of methylene blue to create 0.02mM solution at t=0 and its degradation every 10min up to 60 minutes.

As can be seen in Figure 18, there is not a significant difference between the speed that the dye degraded just by light exposure and the speed when in contact with the radical producing photoelectrodes. This means that the methods the electrodes were produced with were not effective, because if the electrodes were producing the radicals, the dye would have degraded faster than the dye itself being exposed to light. It was also found that the procedure used to produce Bi_2WO_6 could not be scaled up to create an electrode with a thick enough layer so other materials like WO_3 and $BiVO_4$ were tested instead.

4.1.2.   Methyl Orange

A similar test to the methylene blue test was performed, where 20mL of 0.1mM methyl orange in PH7 electrolyte water was placed in front of the solar lamp with no UV filter for 1 hour taking spectrometer readings every 10 minutes up to one hour. The results for this can be seen below in Figure 20:

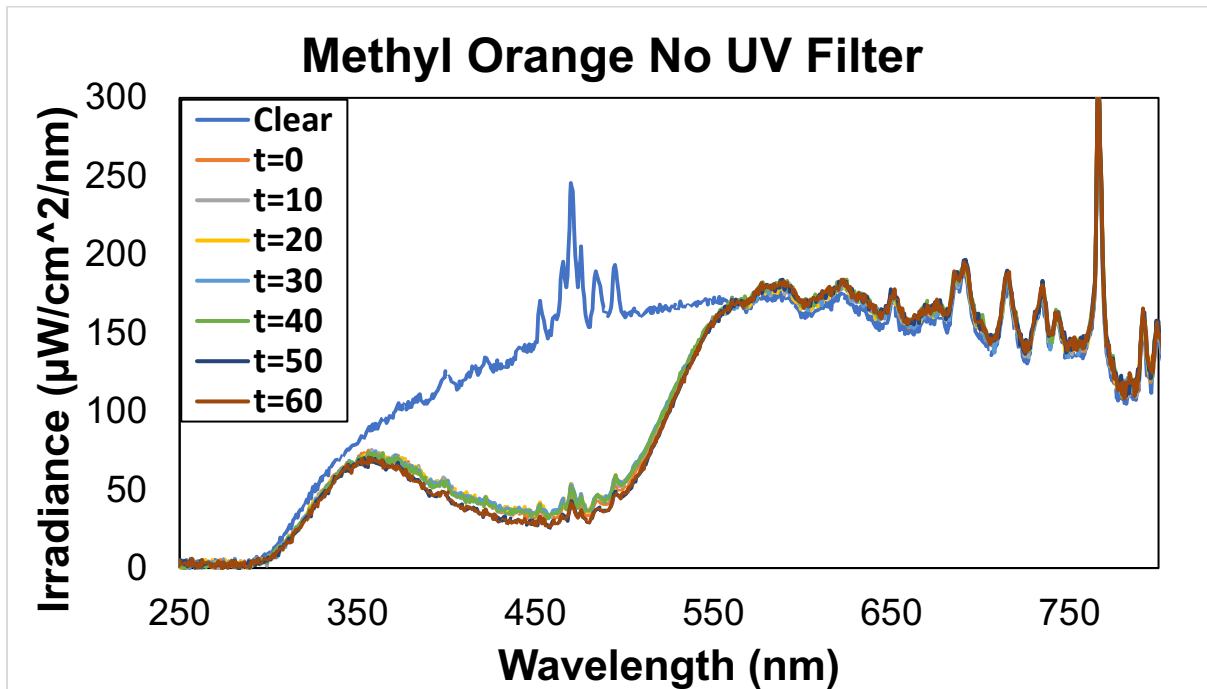*Figure 20: Spectrometer reading of absolute irradiance through the solution from the addition of the dye at t=0 and after 60 minutes.*

The figure shows showed that there was no difference in terms of the irradiance from when the dye was first added and after 60 minutes, meaning that the methyl orange dye is stable in visible light and UV light.

4.2.   Metal Oxide Layer Application Method

The results for each method used to coat both the absorbing and protective metal oxides are outlined below.

4.2.1.   Drop-Coating

The absorbing metal oxides did not adhere well with this method. Dropping the solution of the oxide directly to the FTO glass base spread out well but evaporation was uneven. The image below shows an example of the cells produced with drop coating.

When the solution was dropped it covered the entire area of the cell; however, the final spreading of material during the annealing phase is clearly uneven. This can be seen in the images through the splotching of material. The WO_3 is more prominent in the lower left than it is anywhere else on the cell. This would not maximize the cell's area and would clearly not be a repeatable and consistent method for coatings. This continued to be the case for all other absorbent metal oxide layer solutions. One way that was attempted to resolve this issue was to add a higher volume of liquid to the initial cell.

Figure 21: Cell with 1 layer of WO_3 using drop-coating method. 50 mL of 0.02 M solution dropped onto 2.5 x 2.5cm glass annealed at $500^{O}C$ for 2 hours ramping for 4 hours.

This did help out the amount of material and leave a more even layer. In the attempts however, there was a lot of black residue left on the top of the cell. This may have been coking and when tested in the LSV, the current production was much lower than those of the spin and spray-coated cells. For this reason, other methods of application were chosen instead of drop-coating.

Figure 22: Cell with 1 layer of WO_3 using drop-coating method. 300 mL of 0.05 M solution dropped onto 3 x 1 cm glass annealed at $550^{O}C$ for 2 hours ramping for 4 hours.

The protective metal oxides did not adhere well with this method either. Dropping the solution of the oxide directly to the FTO glass base spread out well but evaporation during the annealing phase was uneven. Figure 23 shows an example of the cells produced with drop coating.

Though this did spread more evenly than the absorbing layer, the protective layer did not, and was therefore not uniform or repeatable. It is clearly seen in Figure 23 that there are thicker or more concentrated areas on the surface of the cell. The same results occurred when attempting with CoO.

Figure 24 shows the comparison between the NiO coated FTO glass and non-coated FTO glass. As can be seen, the layers were uneven when applied and the material distribution on the surface was skewed to one side.
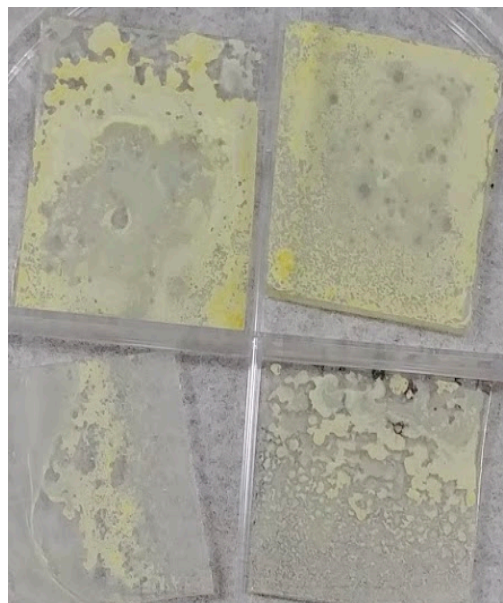

Figure 23: Cells with 1 layer of NiO using drop-coating method. 50mL of 0.05M solution dropped onto 2.5 x2.5cm FTO glass annealed at 350^OC for 3 hours.
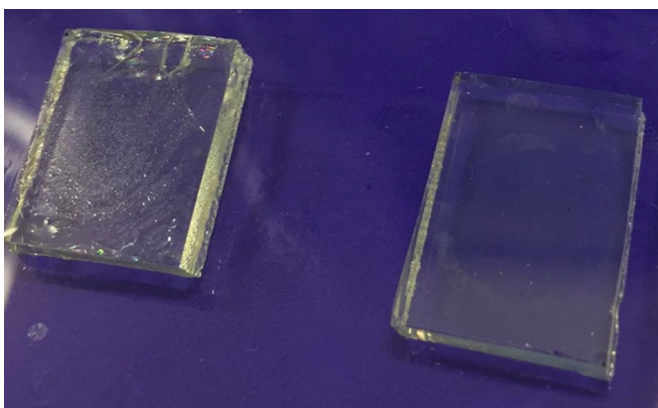
Figure 24: Drop-coated NiO vs. FTO Glass showing uneven distribution of layer onto FTO Glass.

BiVO4 was the only to be synthesized using this method. Drop coating proved to be a good means of synthesizing the BiVO4 cells. For this specific coating, the cells were dropped with material, placed on a hot-plate, heated up, then further annealed in a box furnace. Once this was done, the process was repeated to make more BiVO4 layers on top of the previous ones. For these cells specifically, it is unknown why the spreading worked so much metter than with the other materials. One theory is the higher concentration of the BiVO4 solutions. The higher concentration could have ensured the material was distributed more evenly. The low viscosity of the starting solution and incompatibility with PEG made spin-coating a bad means of application. The specific parameters for making the final cells used for analysis were heating the hot plate up to 500 $^{\text{O}}$C and leaving it for 10 minutes, dropping approximately 50 mL (1-drop) onto the cell, then annealing to 450 $^{\text{O}}$C for 2 hours.

Figure 25: Post annealed SnO₂/BiVO₄ electrodes synthesized using drop-coating

4.2.2.   Dip-Coating

Dip-coating was an improvement to drop-coating the cell. The distribution of material was found to be more consistent than that of the drop-coating method. Less material on the cell allowed for a more even layer to be left after annealing. Figure 27 shows a WO$_3$ cell after it was produced with this method.

Figure 26: Electrode with 1 layer of WO$_3$ using dip-coating method. A 3.5 x 1 cm glass dipped into a 0.2M solution annealed at 550°C for 2 hours ramping for 4 hours with epoxy and wire attached for LSV/CA/Degradation testing.

As can be seen in Figure 26, a large streak of material was left running down the middle. This was a recurring issue when using this method. Often times, due to the dip-speed and orientation in which the cell was dipped, extra material would be left on the cell and therefor spread out unevenly. This was not only seen with the WO$_3$ but also with the other absorbent metal oxides. Though it worked and was effective at making an even layer, the cells would not always be consistent and many were thrown out due to inconsistencies and the presence of unwanted residual material

One way that was attempted to resolve this issue was by adding polyethylene glycol (PEG) to the solution to make it more viscous. Different amounts in various concentrations were added to the solution of absorbing oxides to change the viscosity, but all lead to one of two results. Either not enough was added and the solution and the same original result occurred; or too much was added and the layer burned and turned black. An example of this can be seen in Figure 27.

Figure 27: Cell with 1 burned layer of WO3 + PEG using dip-coating method. A 3.5 x 3 cm glass dipped into a 0.2M solution annealed at 550°C for 2 hours ramping for 4 hours.

4.2.3.   Spray-Coating

Figure 28: Cell with 1 layer of WO₃ using spray-coating method. A 3.5 x 1 cm glass sprayed with a 0.2M solution and 1 spray ~13mL annealed at 550°C for 2 hours ramping for 4 hours.

Spray-coating was found to be more effective than dip-coating. As can be seen in Figure 28, spray coating achieved a nearly even layer that spread throughout the cell's entire area. Some splotching was seen throughout the cell, but it was generally even and well distributed.

The issue that arose is that when applying the spray for more than one layer, is the glass would often break. This was due to the sprayed solution being significantly colder than that of the glass it was being applied to. After just 2 coatings, the glass would begin to crack and would affect the integrity of the cells. To address this, the annealing temperature were lowered with the protective layer oxides as they did not need to be as high of a temperature as the absorbing metal oxides.

Figure 29 shows a glass-cell after being spay coated with a solution of 0.05 M Nickel Chloride to make Nickel Oxide.

As can be seen in Figure 29, the spray coating technique deposited a clear and even layer on-top of the glass. These cells will also be analyzed to determine whether the material is Nickel Oxide and how evenly distributed it is on top of the glass. The thickness, according to this method and literature, is approximately 20 nm. This procedure seemed to work much better for the protective coatings than it did for the absorbing metal oxides at lower temperatures.
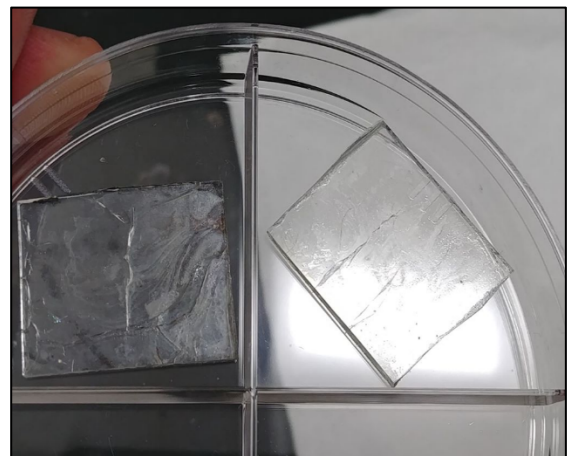
Figure 29: Cell with 1 layer of NiO using spray-coating method. A 3.5 x 3 cm glass sprayed with a 0.05M solution and 1 spray ~13mL 4mL/min annealed at 350°C on a hot plate.

Due to the issue of the glass breaking with the absorbing metal oxides, the application method was changed. Such changes were to wait for the cell to completely cool before applying another layer and to add more sprays (more volume) of material to each coating. More issues arose with these new changes. The spray did not adhere well to the previous layer and splotching was seen around the cell. The coating seemed to only adhere evenly either when the cell was hot, or when it was being applied directly to the FTO glass. Due to the inability to easily add more layers to the cell and general processability, this method was not adopted into common application of cell layers.
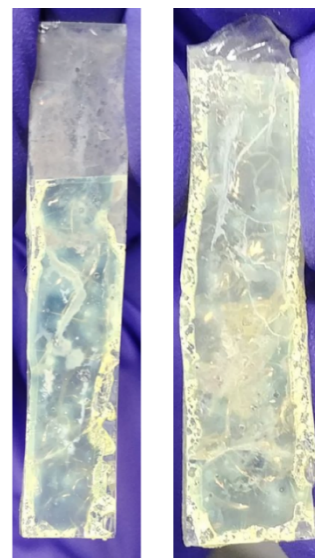

Figure 30: Cell with 2 (left) & 3 (right) layers of WO₃ using spray-coating method. A 3.5 x 1 cm glass sprayed with a 0.2M solution and 1 spray ~13mL annealed at 550°C for 2 hours ramping for 4 hours between coatings.

4.2.4.   Spin-Coating

Spin coating was the most successful of all coating methods. It accomplished the most evenly coated layers for both the absorbing and protective layers. The process for coating each layer is dependent on many variables; spin-speed, initial material, and annealing temperatures.

TiO2 was the first coating to be developed. After adjusting the spin speeds and relative quantity of dropped material a good range of starting values for spin-speed, dropping amount, and annealing temperature were found. For the TiO2 solution, the ideal spin speeds were found to be between 2,000 and 3,000 rotations per minute (RPM). It was also found that most of the materials used in this MQP oxidize above 500 ^{O}C; therefore, the annealing temperature was chosen to be 550 ^{O}C. The TiO2 specifically, was spun at 3,000 RPM for 15 seconds and produced a layer approximately 1 micron thick. The amount dropped as 300 microliters, enough to cover the whole are of the cell before it was spun.

Figure 31: 1micron thick TiO$_2$ coated FTO glass.

 WO3 was the next material to be successfully synthesized with the spin-coating method as can be seen in Figure 32. This material was more difficult as the viscosity of the initial solution was less viscous. Eventually, polyethylene glycol was added to the solution to increase the viscosity and allow the material to spread more evenly. The final parameters were a spin speed of 3,000 RPMs for 15 seconds, 300 microliters of solution, and an annealing temperature of 550 ^{O}C with a 4-hour ramp and 2-hour hold at the final temperature.

Figure 32: WO$_3$ coated FTO glass

Both protective coatings were also applied using spin-coating. Both started off as solutions such as the one pictured in figure 34. The NiO coatings and CoO coatings both used very similar parameters. Those parameters are as follows: spin-speed 3,000 RPM for 50 seconds, 300 microliters of material dropped prior to spinning, annealing to 500 ^{O}C ramped for 1.5 hours and held for 2. Figure 33 shows spin coated BiVO$_4$ cells with CoO and NiO respectively.

Figure 33: Nickel Chloride solution used to synthesize synthetic coating
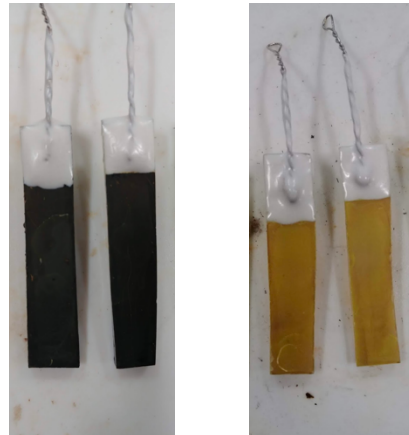

Figure 34: CoO (left) & NiO (right) Coated BiVO4 Cells using spin-coating

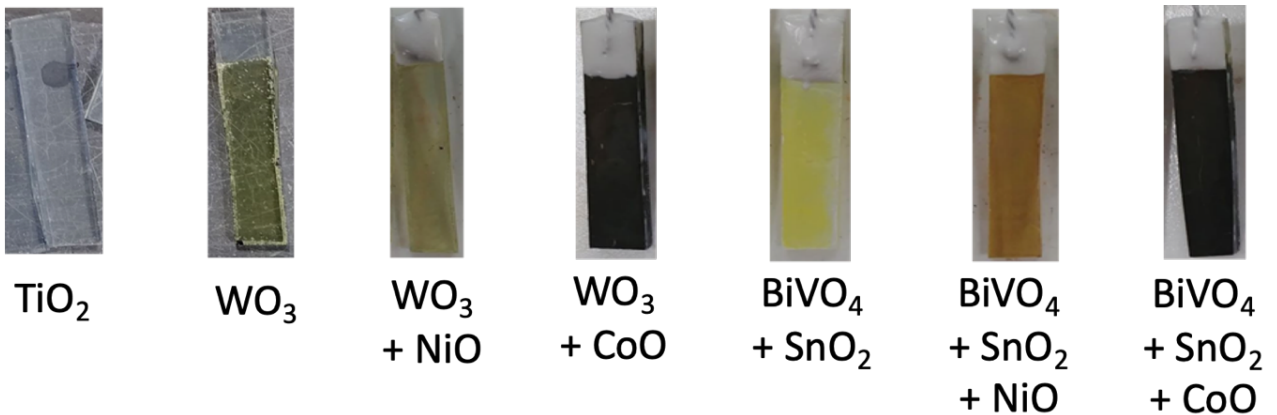Figure 34 below shows a final outline of all the cell variations produced.

TiO$_2$ WO$_3$ WO$_3$ + NiO WO$_3$ + CoO BiVO$_4$ + SnO$_2$ BiVO$_4$ + SnO$_2$ + NiO BiVO$_4$ + SnO$_2$ + CoO

Figure 35: Pictures of the seven electrodes using final application methods.

4.3.   Current Efficiency

Figure 36 below summarizes of results for the LSV test of the WO_3 electrodes with and without protective coatings compared with TiO_2. The individual results for each type of electrode can be found in Appendix B.
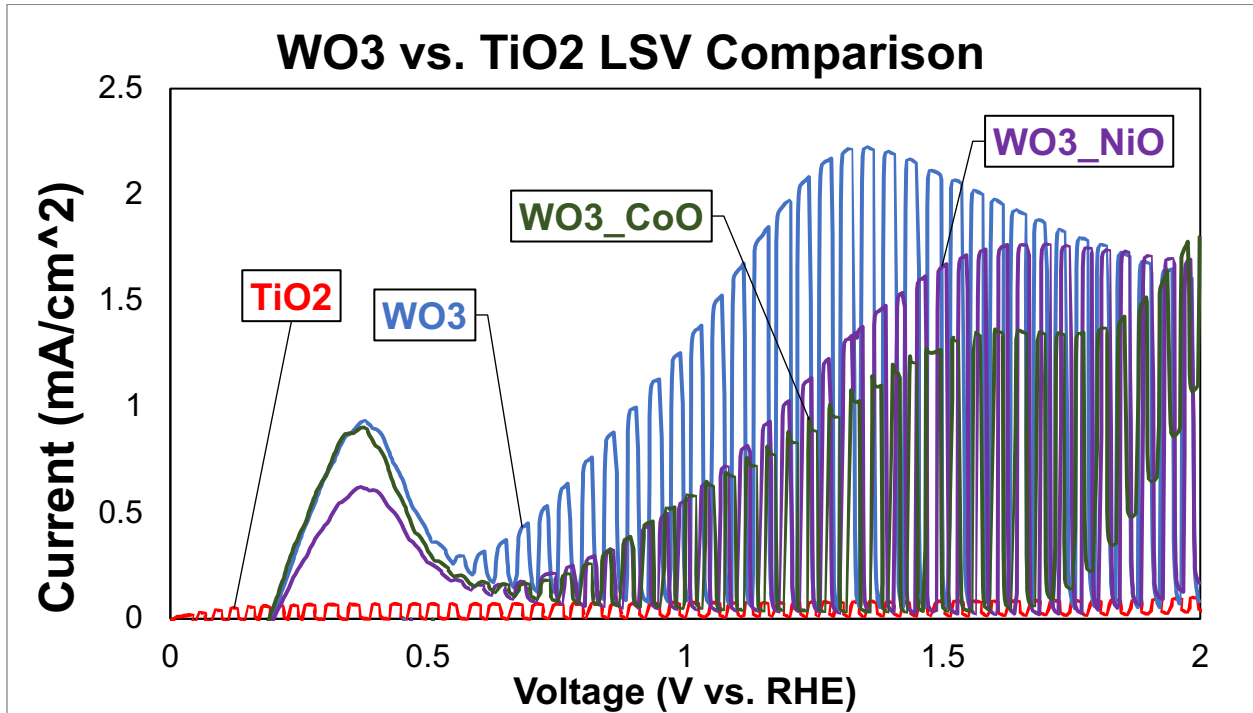

Figure 36: LSV from 0-2V vs. RHE in 20mL of PH7 electrolyte solution of WO_3 electrodes with and without protective coatings compared with TiO_2

It is clear that the all of the WO_3 electrodes produce significantly more current than the TiO_2 electrode. The peak of the WO_3 electrode even induced 33x more current than the TiO_2 electrode. Although it would be expected that the protective coatings would act as a p-type electrode in reference to the n-type WO_3 reducing the voltage requirements to produce the same current, the opposite was observed. The shift to the right, meaning the electrodes requiring a higher applied current to drive the reaction, may mean that NiO and CoO do not act as p-type electrodes with WO_3, or that WO_3 is driving a separate reaction with the electrolyte solution causing there to be a spike in current at the lower voltage.

Figure 37 below summarizes of results for the LSV test of the BiVO$_4$ electrodes with and without protective coatings compared with TiO$_2$.
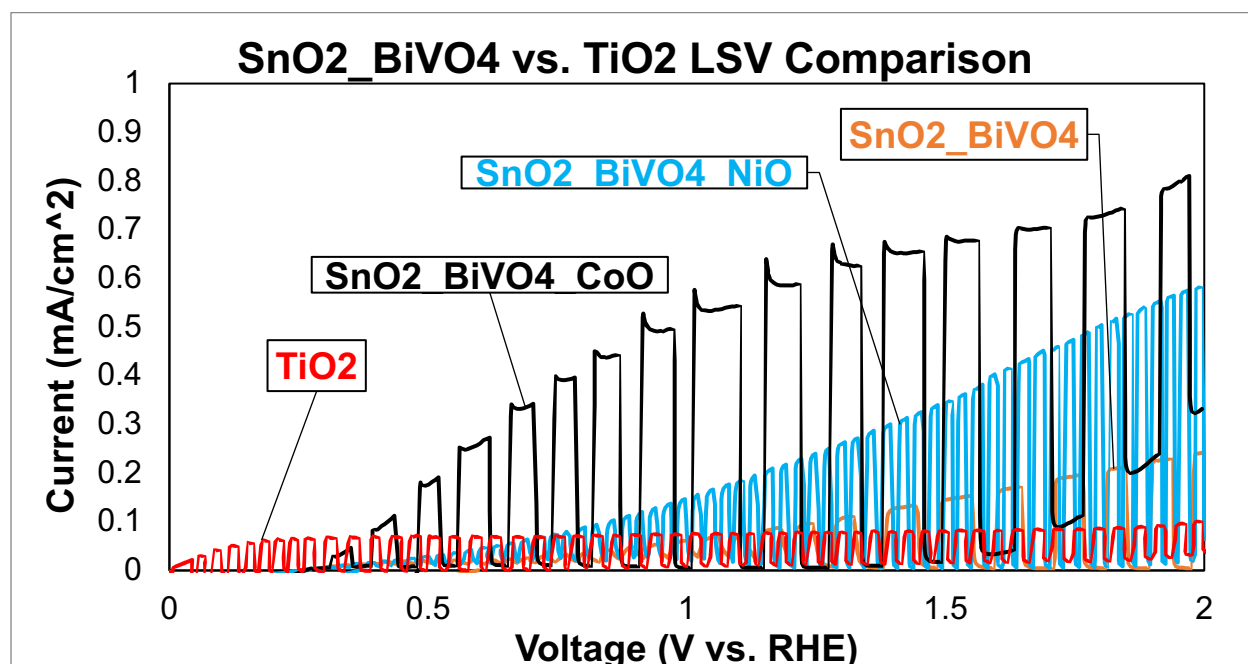

Figure 37: LSV from 0-2V vs. RHE in 20mL of PH7 electrolyte solution of WO$_3$ electrodes with and without protective coatings compared with TiO$_2$

The SnO$_2$/BiVO$_4$ electrodes with and without protective coatings also produced more current than the TiO$_2$ though less than WO$_3$. The base SnO$_2$/BiVO$_4$ electrode without protective coatings only produced more current than TiO$_2$ after 1.1V, whereas the SnO$_2$/BiVO$_4$/NiO produced more current starting at around 0.7V and SnO$_2$/BiVO$_4$/CoO produced more current starting around 0.4V. This means the NiO and CoO protective coatings did reduce the voltage requirements to drive the reaction as would be expected with the SnO$_2$/BiVO$_4$ acting as an n-type electrode and the NiO and CoO as a p-type.

47

4.4.   Stability of Electrodes

Figure 38 below summarizes the results of the CA tests used to test stability.
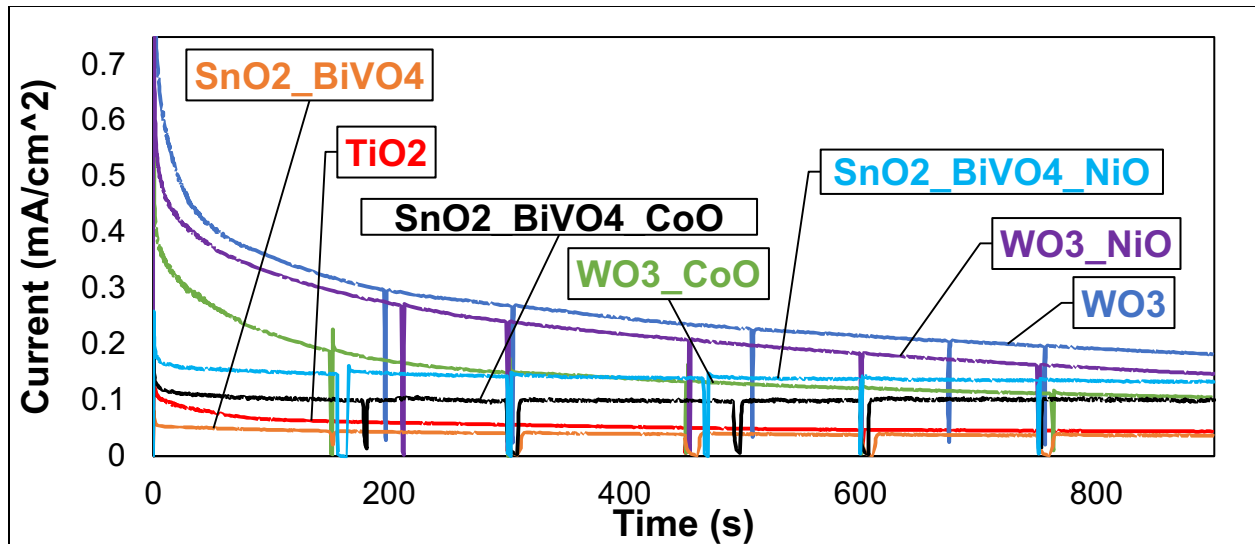

Figure 38: Summary of CA stability tests in 20mL PH7 electrolyte solution in beaker for 15min at 0.343V vs. SCE (1V vs. RHE).

Figure 39 focuses on the CA results for the WO_3 electrodes with and without coatings compared with TiO_2. In the case of WO_3, the protective coatings were not very effective at preventing the degradation of the electrode. This result may just be due to the short time scale of 15min and would present differently after 1hour testing a degradation.
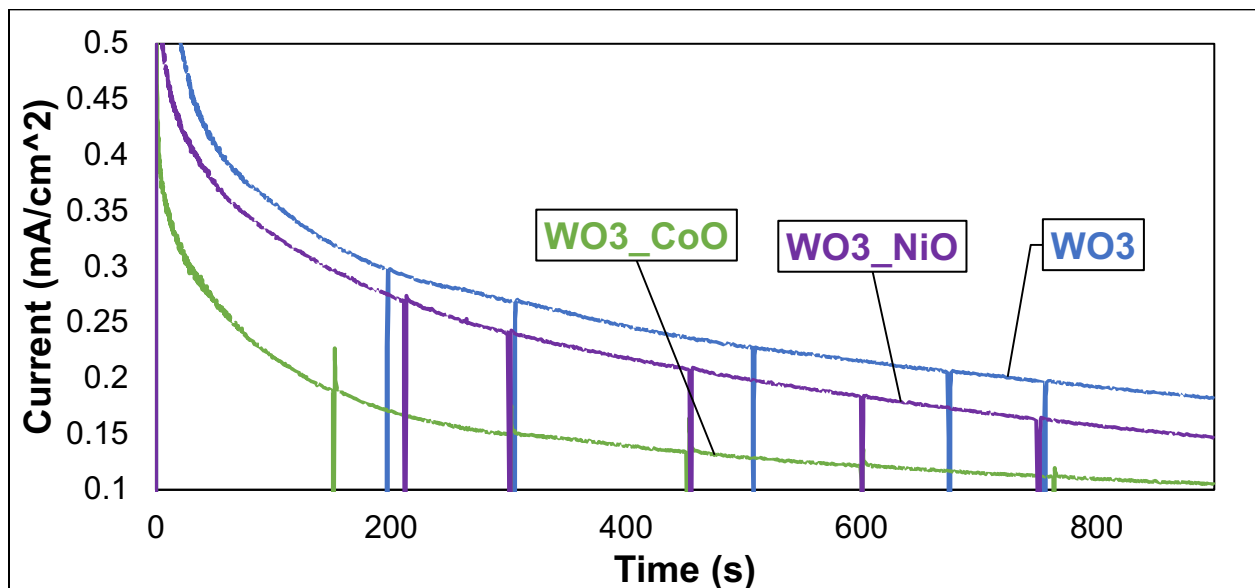

Figure 39: Comparison of CA for WO_3 electrodes with and without protective coatings for 15min.

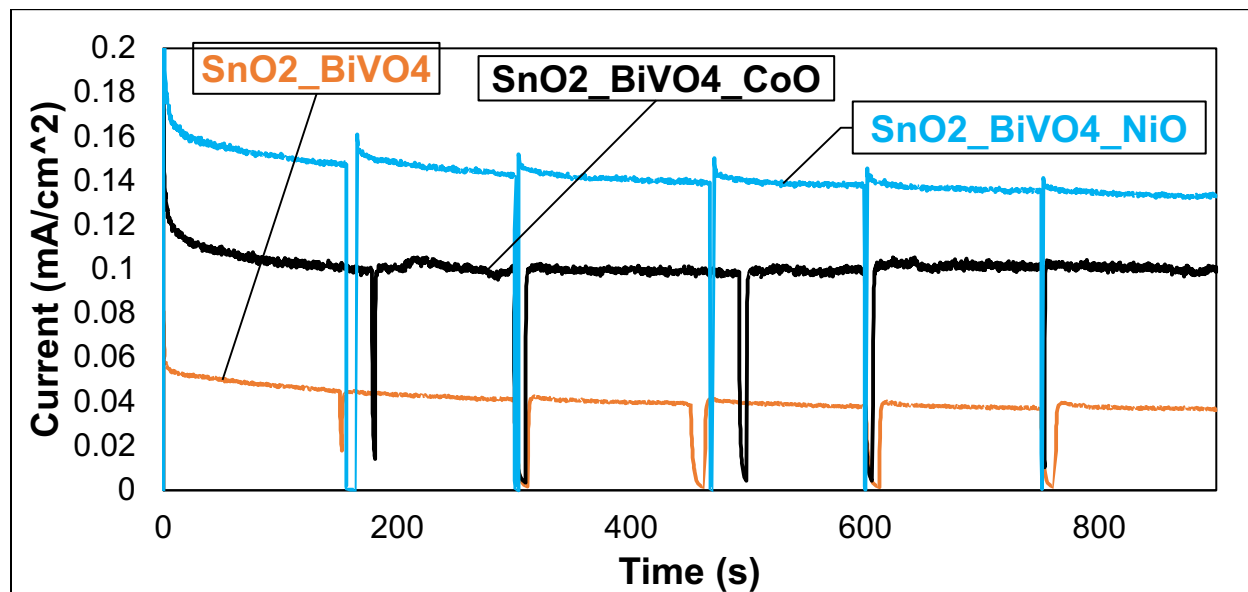Figure 40 below shows the similar comparison of the BiVO$_4$ electrodes.

Figure 40: Comparison of CA for BiVO$_4$ electrodes with and without protective coatings for 15min.

Unlike WO$_3$, the protective coatings did show better protection of the electrode, especially CoO. The CoO coating kept the current almost exactly the same throughout the 15 minutes, and perhaps this would continue if the electrode were tested for a longer amount of time like for an hour.

4.5.   Degradation

Following the Cuvette Dye Degradation procedure described in Section 3.5.3, TiO_2, WO_3, and $BiVO_4$ electrodes were tested and it was found that $BiVO_4$ was the most effective at degrading the organic methyl orange dye. A summary of the results can be seen below in Figure 41, and the spectrometer readings used to calculate the extent of degradation can be found in Appendix A.
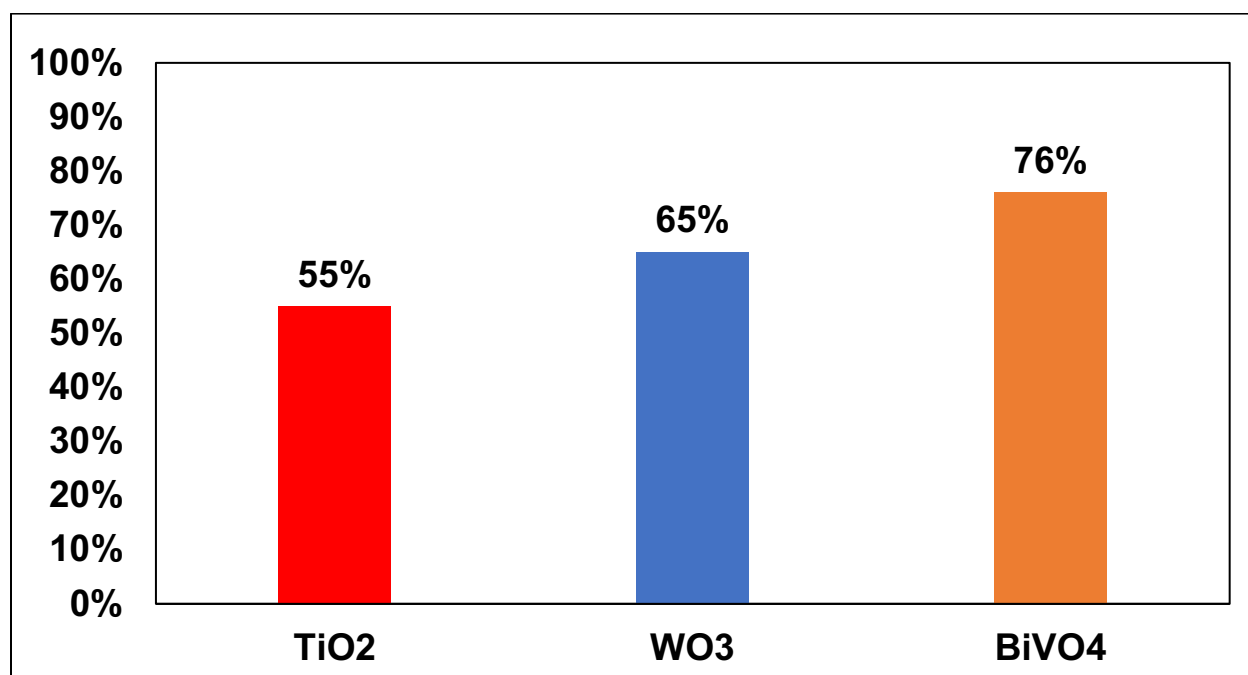

Figure 41: Extent of degradation of 3mL of 0.02mM solution methyl orange dye in PH7 electrolyte after 1hr with 1V applied for TiO_2, WO_3, and $BiVO_4$ electrodes.

The TiO_2 degraded the least amount of the least amount of the dye after 1hr even though it had $3.2cm^2$ of surface area compared to the WO_3 and $BiVO_4$ electrodes which had only $2.96cm^2$ of surface area. The extent of degradation is not normalized to the relative surface areas of the cell, however, it is clear that TiO_2 degraded less with more surface area.

5. Conclusions and Future Work

The LSV data shows that WO_3 and $BiVO_4$ are significantly more efficient than TiO_2 when exposed to the same light conditions suggesting they can absorb visible light wavelengths to overcome the band gap. Because the test conditions were kept the same for the tests, the only difference could be that the WO_3 and BiVO4 electrodes are absorbing wavelengths of visible light and they must be overcoming the band gap because the current is higher than in TiO_2 at the same voltage meaning more electrons are being excited into the conduction band.

The CA data showed that the WO_3 and $BiVO_4$ electrodes without protective coatings did degrade over time because the induced current reduced significantly over time. The protective coatings layered over the $BiVO_4$ were effective at preventing the current from reducing over time; however, they did not prevent it for WO_3. The protective coatings over $BiVO_4$ also shifted the voltage requirements for similar current efficiency so that lower voltages were required to get similar current levels. The coatings caused the WO_3 voltage requirements to shift requiring more voltage for similar current levels. This suggests that the protective coatings were effective at creating an n-type electrode where the valence electrons in $BiVO_4$ were transferred to the positive holes of NiO and CoO, but did not create such an electrode with WO_3. Furthermore, the early spike in current at a lower voltage with WO_3 without protective coatings could be caused by the WO_3 reacting with the potassium monobasic and potassium dibasic used to create the PH7 electrolyte solution.

Both WO_3 and $BiVO_4$ had higher extents of dye degradation than TiO_2 using the same testing conditions, which suggests that they are more effective at degrading organic contaminants. This means that WO_3 produces more of the hydroxyl and superoxide radicals than TiO_2. It also suggests that hydrogen peroxide might be more effective at organic degradation than the radicals since the $BiVO_4$ degraded the most.

Future work involving these coatings may include focusing on improving the efficiency of the electrodes by improving the surface area of the metal oxide. This could be done by producing metal oxide layers with different nanostructures like branched nanorods. Efficiency can be further improved by utilizing a layer of mesoporous SnO_2 instead of compact SnO_2 on both the $BiVO_4$ and the WO_3. The protective coating procedures should also be improved because only nominal improvements of electrode stability were observed but published papers have shown their effectiveness at maintaining current levels for hours. More research into the unexpected results of the protective coatings application to WO_3 electrodes should be done because theoretically they should have reduced the required applied current needed to drive the reaction, not increase it. Finally, once a more optimized electrode has been produced, a prototype water bottle should be designed to test the final goal of this research.

6. References

1.   Jones, M. Five Methods to Purify Water from a Military Survival Instructor. https://thenewsrep.com/70472/five-methods-purify-water-military-survival-instructor/ (accessed 03/30/19).
2.   Curtis, R. OA Guide to Water Purification. http://www.princeton.edu/~oa/manual/water.shtml.
3.   McCarthy, P. Solar Water Purification: Misconceptions and Facts. https://www.offgridweb.com/survival/solar-water-purification-misconceptions-and-facts/.
4.   Donal A. Keane, K. G. M., Pilar Fernandez Ibañez, M. Inmaculada Polo-Lopez, J. Anthony Byrne, Patrick S. M. Dunlop, Kevin O'Shea, Dionysios D. Dionysiou, Suresh C. Pillai, Solar Photocatalysis for water disinfection materials and reactor design. *Catalysis Science & Technology* **2014,** *4*, 1211.
5.   AL., G. T. E., THE SOLAR SPECTRAL IRRADIANCE FROM 200 TO 2400 nm AS

MEASURED BY THE SOLSPEC SPECTROMETER FROM THE ATLAS

AND EURECA MISSIONS. *Solar Physics 214: 1–22, 2003* **2003,** *214*, 1-22.
6.   Chan, S. H. S.; Yeong Wu, T.; Juan, J. C.; Teh, C. Y., Recent developments of metal oxide semiconductors as photocatalysts in advanced oxidation processes (AOPs) for treatment of dye waste-water. *Journal of Chemical Technology & Biotechnology* **2011,** *86* (9), 1130-1158.
7.   EPA Learn about Decontamination for Drinking Water and Wastewater Utilities. https://www.epa.gov/waterutilityresponse/learn-about-decontamination-drinking-water-and-wastewater-utilities (accessed 10/11/2018).
8.   Malato, S.; Fernández-Ibáñez, P.; Maldonado, M. I.; Blanco, J.; Gernjak, W., Decontamination and disinfection of water by solar photocatalysis: Recent overview and trends. *Catalysis Today* **2009,** *147* (1), 1-59.
9.   Deng, Y.; Zhao, R., Advanced Oxidation Processes (AOPs) in Wastewater Treatment. *Current Pollution Reports* **2015,** *1* (3), 167-176.
10.   Rao, P., Metal Oxide Photoelectrodes for Solar-Driven Water Decontamination. **2018.**
11.   Patra, D. Titanium Dioxide. https://www.britannica.com/science/titanium-dioxide.
12.   Stylidi, M., Pathways of solar light-induced photocatalytic degradation of azo dyes in aqueous TiO2 suspensions. *Applied Catalysis B: Environmental* **2003,** *40* (4), 271-286.
13.   Ammar Houas, H. L., Mohamed Ksibi, Elimame Elaloui, Chantal Guillard, Jean-Marie Herrmann, Photocatalytic degradation pathway of methylene blue in water. *Appl Catal B-Environ* **2001,** *31* (2), 145-157.
14.   Nakata, K.; Fujishima, A., TiO2 photocatalysis: Design and applications. *J Photoch Photobio C* **2012,** *13* (3), 169-189.
15.   Dong, S.; Feng, J.; Fan, M.; Pi, Y.; Hu, L.; Han, X.; Liu, M.; Sun, J.; Sun, J., Recent developments in heterogeneous photocatalytic water treatment using visible light-responsive photocatalysts: a review. *RSC Advances* **2015,** *5* (19), 14610-14630.
16.   Baek, J. H.; Gill, T. M.; Abroshan, H.; Park, S.; Shi, X.; Nørskov, J.; Jung, H. S.; Siahrostami, S.; Zheng, X., Selective and Efficient Gd-Doped BiVO4 Photoanode for Two-Electron Water Oxidation to H2O2. *ACS Energy Letters* **2019,** *4* (3), 720-728.
17.   Xu, Y.; Schoonen, M. A. A., The absolute energy positions of conduction and valence bands of

selected semiconducting minerals. *American Mineralogist* **2000,** *85*, 543-556.

18. Hu, S.; Lewis, N. S.; Ager, J. W.; Yang, J. H.; McKone, J. R.; Strandwitz, N. C., Thin-Film Materials for the Protection of Semiconducting Photoelectrodes in Solar-Fuel Generators. *J Phys Chem C* **2015,** *119* (43), 24201-24228.

19. Cambridge, C. E. B. F. o. t. U. o. Linear Sweep and Cyclic Voltametry: The Principles. https://www.ceb.cam.ac.uk/research/groups/rg-eme/Edu/linear-sweep-and-cyclic-voltametry-the-principles.

20. Chemistry, R. S. o. Chrono-amperometry. https://www.rsc.org/publishing/journals/prospect/ontology.asp?id=CMO:0000005&MSID=c3cp44313b.

21. Khataee, A. R.; Pons, M. N.; Zahraa, O., Photocatalytic degradation of three azo dyes using immobilized TiO2 nanoparticles on glass plates activated by UV light irradiation: influence of dye molecular structure. *J Hazard Mater* **2009,** *168* (1), 451-7.

22. Zou, Y.; Gong, Y.; Lin, B.; Mellott, N. P., Photodegradation of methylene blue in the visible spectrum: An efficient W6+ ion doped anatase titania photocatalyst via a solvothermal method. *Vacuum* **2016,** *126*, 63-69.

23. Prahl, S. Methylene Blue Spectra. (accessed 9/19/2018).

24. Magureanu, M.; Mandache, N. B.; Parvulescu, V. I., Degradation of organic dyes in water by electrical discharges. *Plasma Chem Plasma P* **2007,** *27* (5), 589-598.

25. Zyoud, A.; Zu'bi, A.; Helal, M. H.; Park, D.; Campet, G.; Hilal, H. S., Optimizing photo-mineralization of aqueous methyl orange by nano-ZnO catalyst under simulated natural conditions. *J Environ Health Sci Eng* **2015,** *13*, 46.

26. Gomez, L.; Sebastian, V.; Arruebo, M.; Santamaria, J.; Cronin, S. B., Plasmon-enhanced photocatalytic water purification. *Phys Chem Chem Phys* **2014,** *16* (29), 15111-6.

27. Patil, P. S.; Kadam, L. D., Preparation and characterization of spray pyrolyzed nickel oxide (NiO) thin films. *Applied Surface Science* **2002,** *199* (1-4), 211-221.

28. San Vicente, G.; Morales, A.; Gutierrez, M. T., Preparation and characterization of sol–gel TiO2 antireflective coatings for silicon. *Thin Solid Films* **2001,** *391* (1), 133-137.

29. Rout, T.; Bera, S.; Udayabhanu, G.; Narayan, R., Methodologies of Application of Sol-Gel Based Solution onto Substrate: A Review. *Journal of Coating Science and Technology* **2016,** *3* (1), 9-22.

30. Raj Das, A. C., Fabrication and Properties of Spin-Coated Polymer Films. *Nano-size polymers: Preparation, properties, applications* **2016**, 283-306.

31. Ricci, R. W.; Ditzler, M. A.; Nestor, L. P., Discovering the Beer-Lambert Law. *Chemical Education Today* **1994,** *Volume 71*.

7. Appendix

7.1.   Appendix A: Dye Efficacy Spectrometer Data

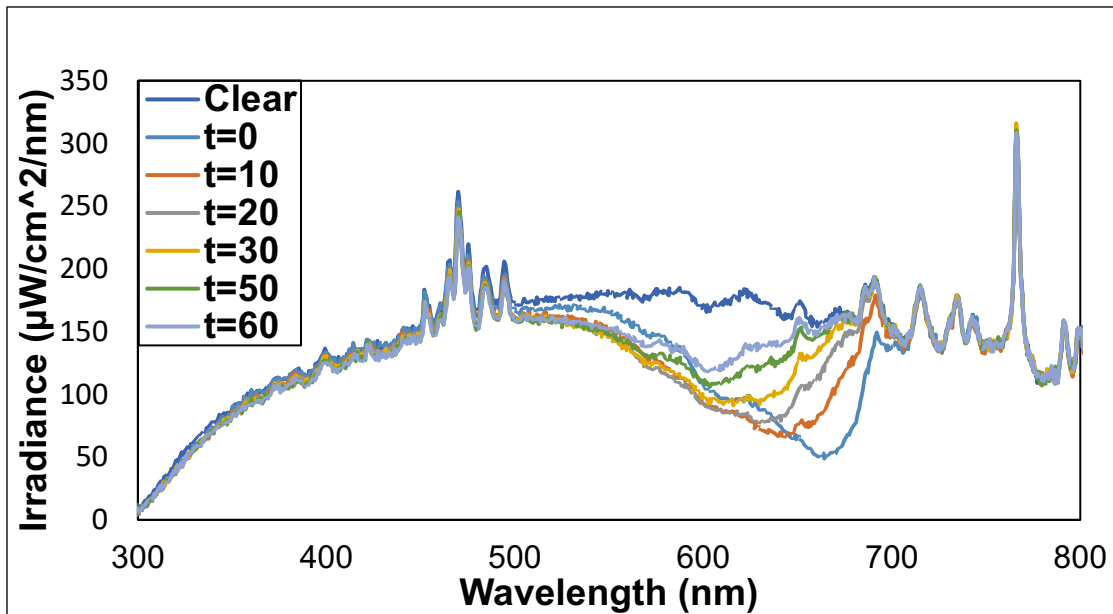### 7.1.1 Methylene Blue in UV and Visible Light

Figure 42: 20mL of 0.01mM Methylene Blue 7PfH in Solar Lamp for 1hr.
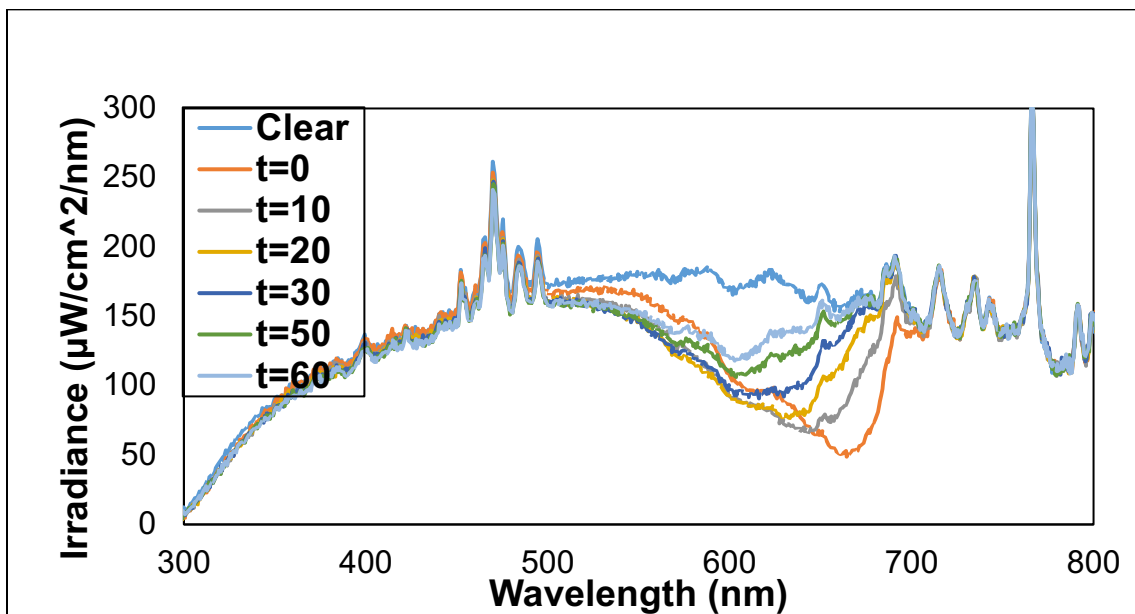
7.1.2 Methylene Blue in Visible Light

Figure 43: 20mL of 0.01mM Methylene Blue 7PH in Visible Light for 1hr.
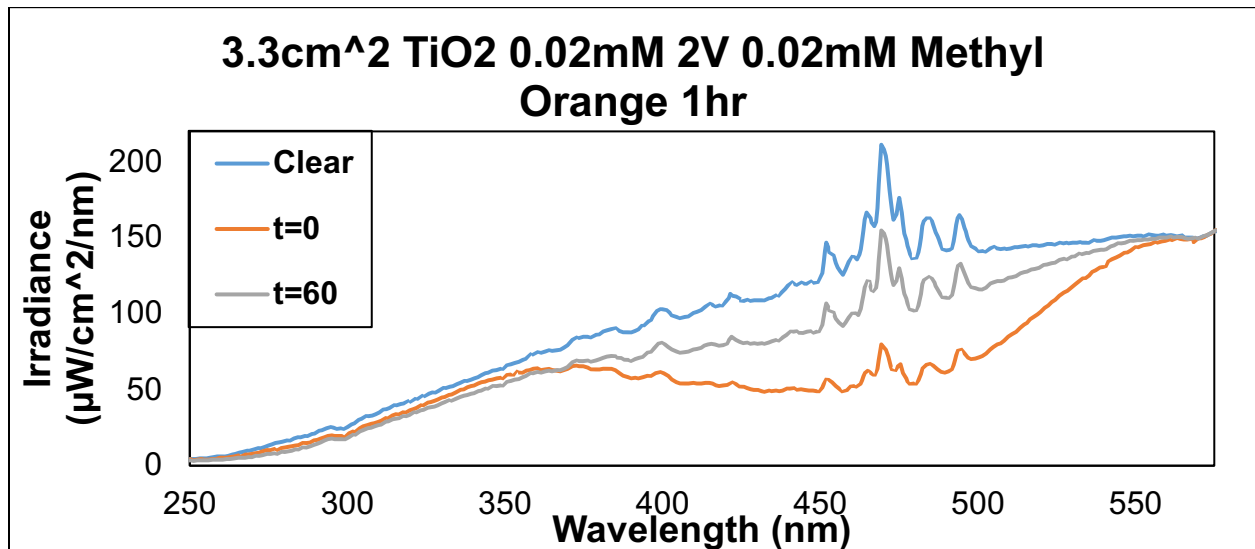
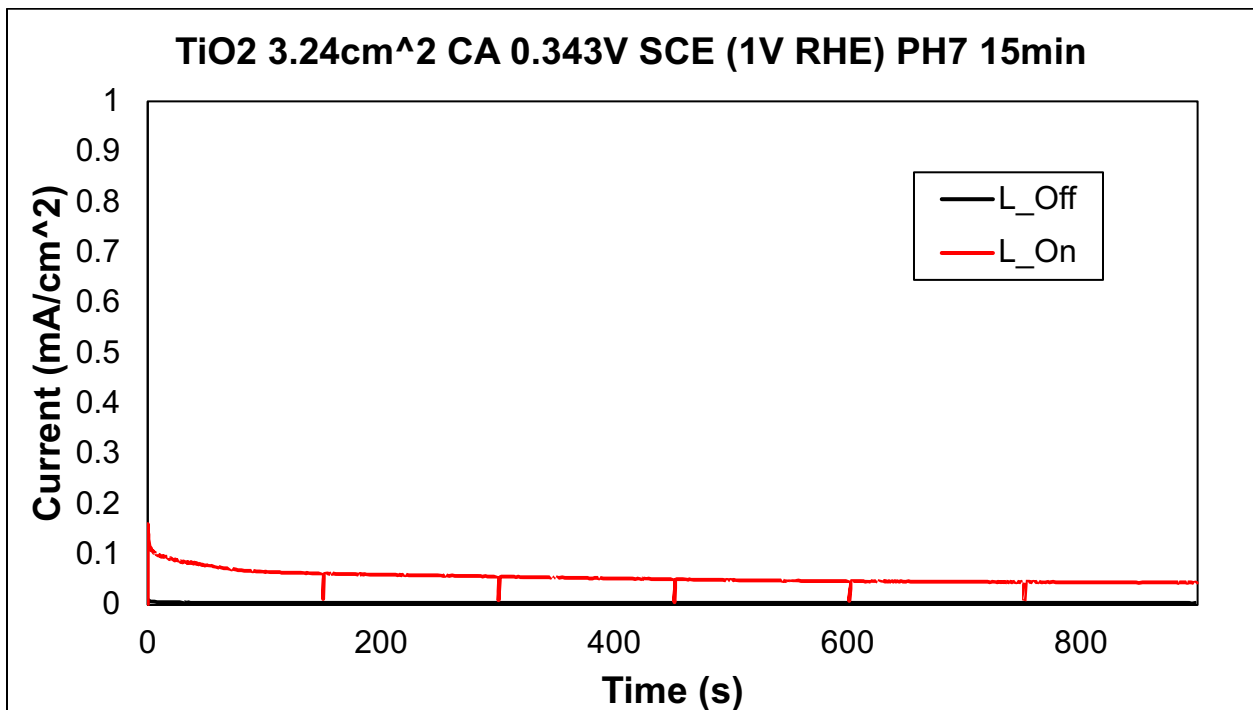## 7.2.   Cuvette Degradation Spectrometer Results
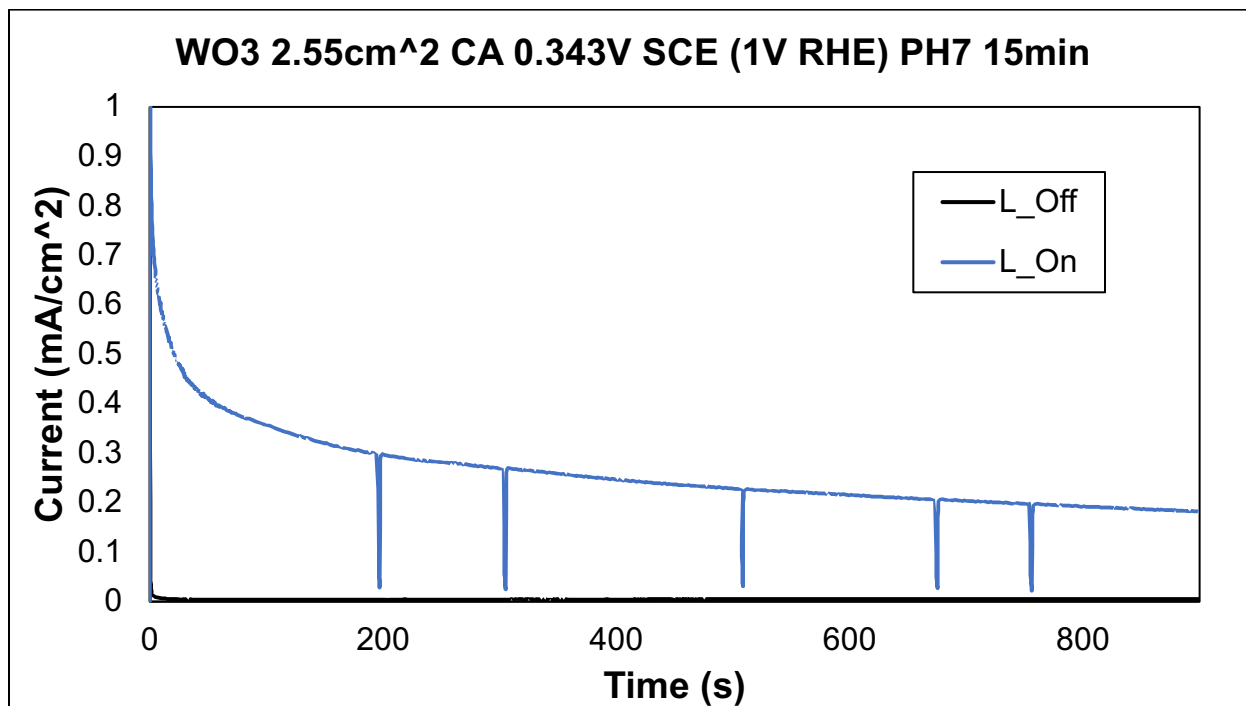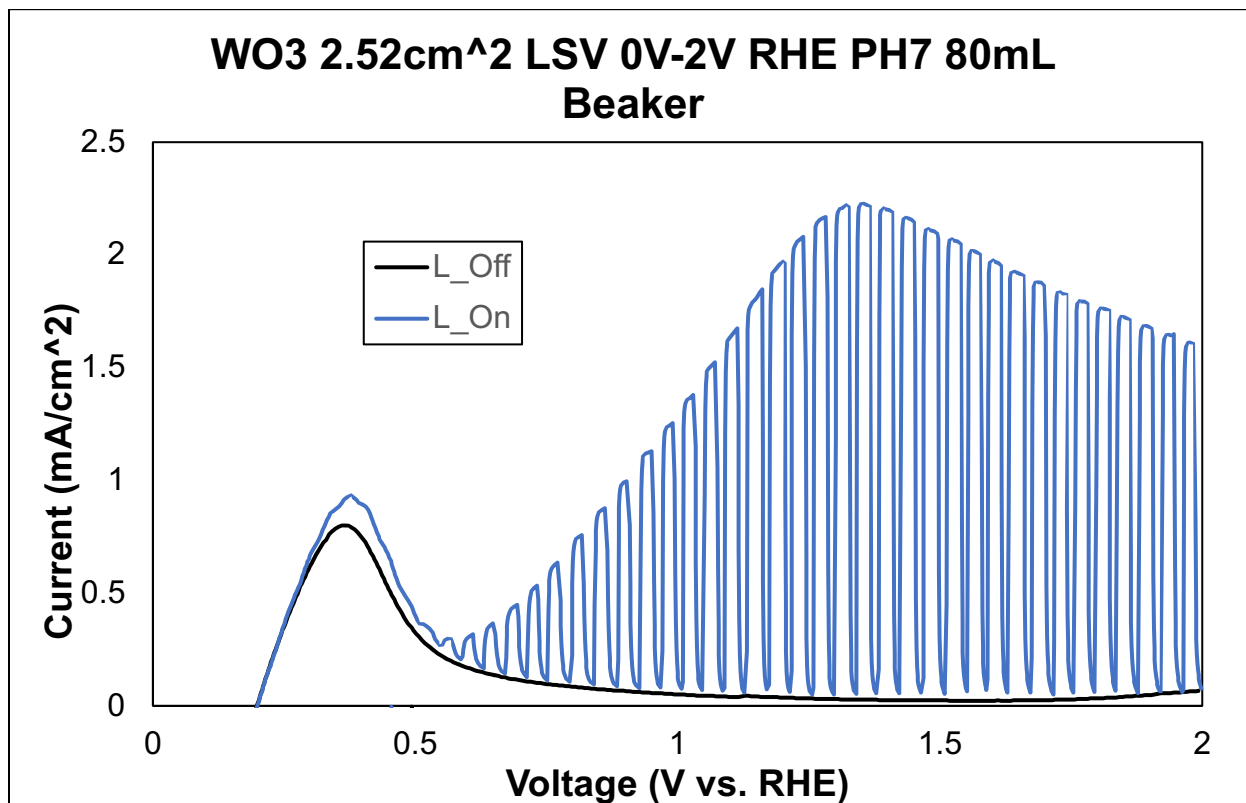
7.2.1 TiO$_2$

Figure 44: Spectrometer data of 3mL of 0.02mM Methyl Orange dye in 7PH electrolyte solution degradation after 1hour with TiO$_2$ electrode using Cuvette Dye Degradation procedure.

7.2.2 WO$_3$
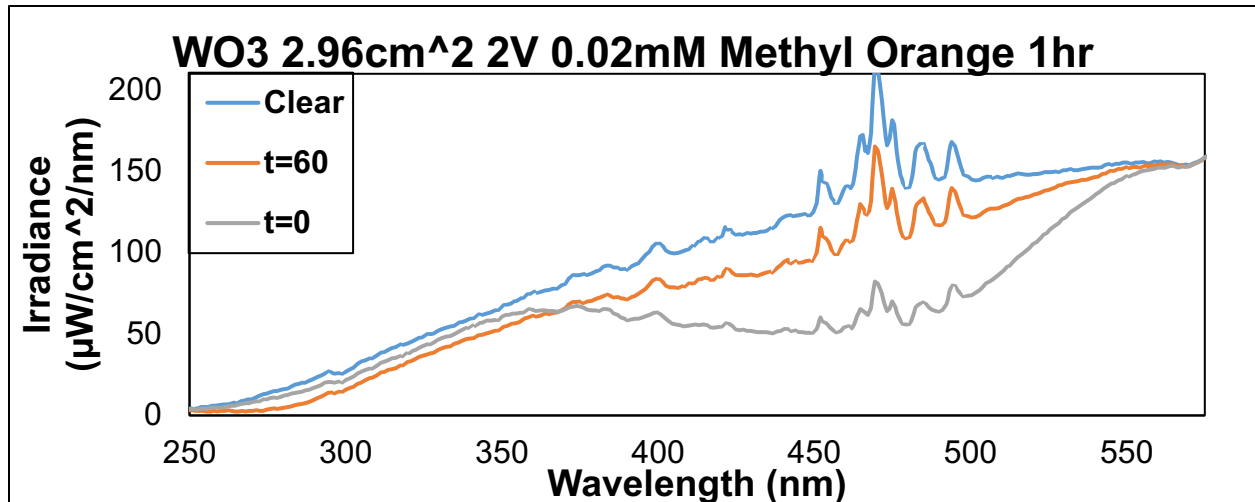
Figure 45: Spectrometer data of 3mL of 0.02mM Methyl Orange dye in 7PH electrolyte solution degradation after 1hour with WO$_3$ electrode using Cuvette Dye Degradation procedure.
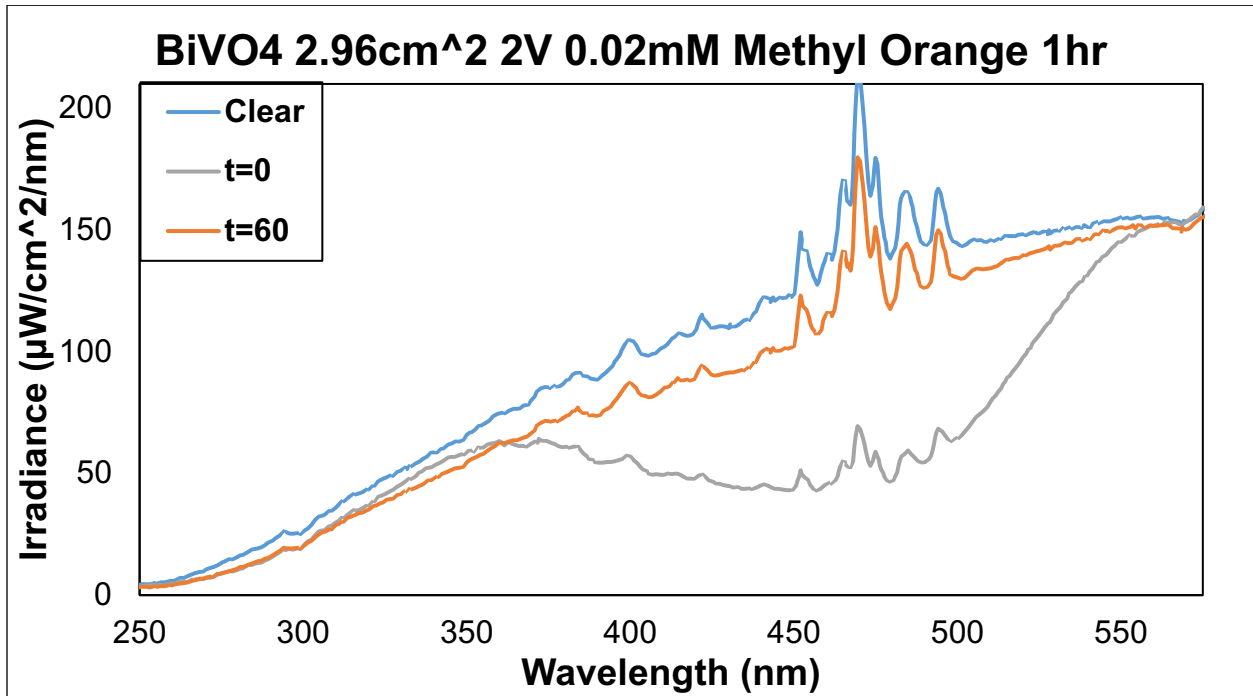
Figure 46: Spectrometer data of 3mL of 0.02mM Methyl Orange dye in 7PH electrolyte solution degradation after 1hour with BiVO₄ electrode using Cuvette Dye Degradation procedure.
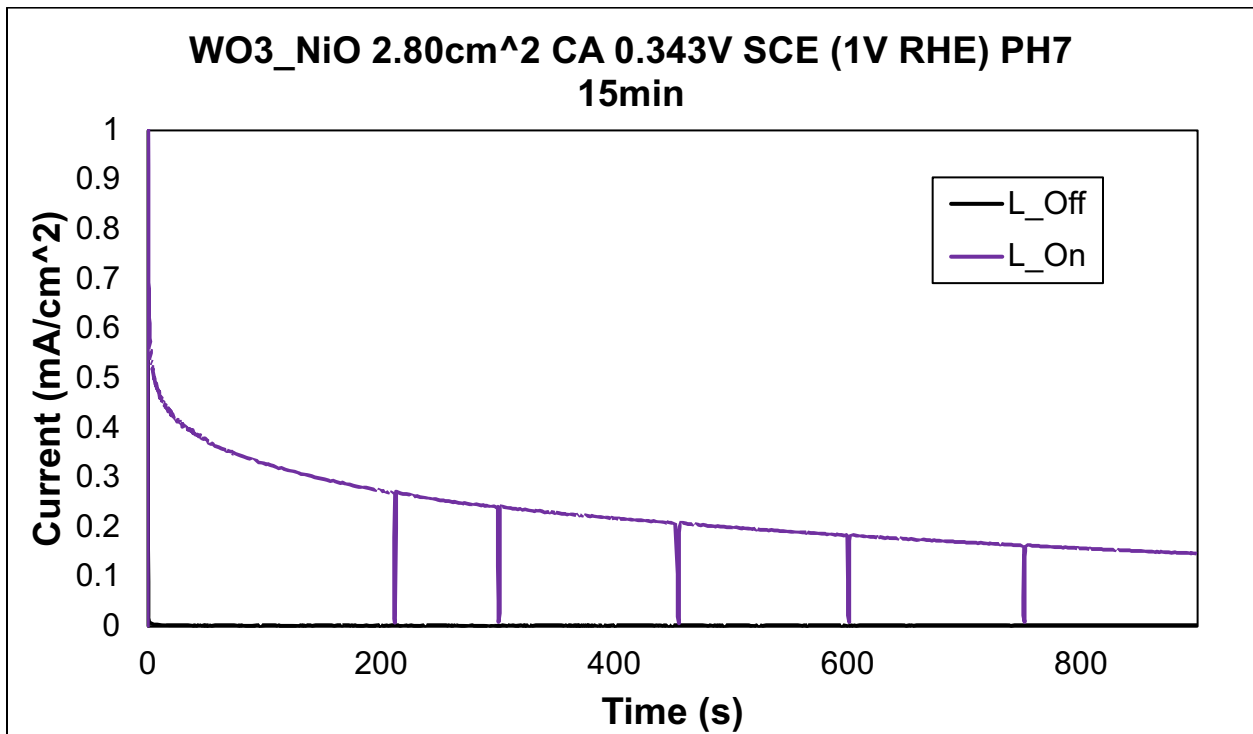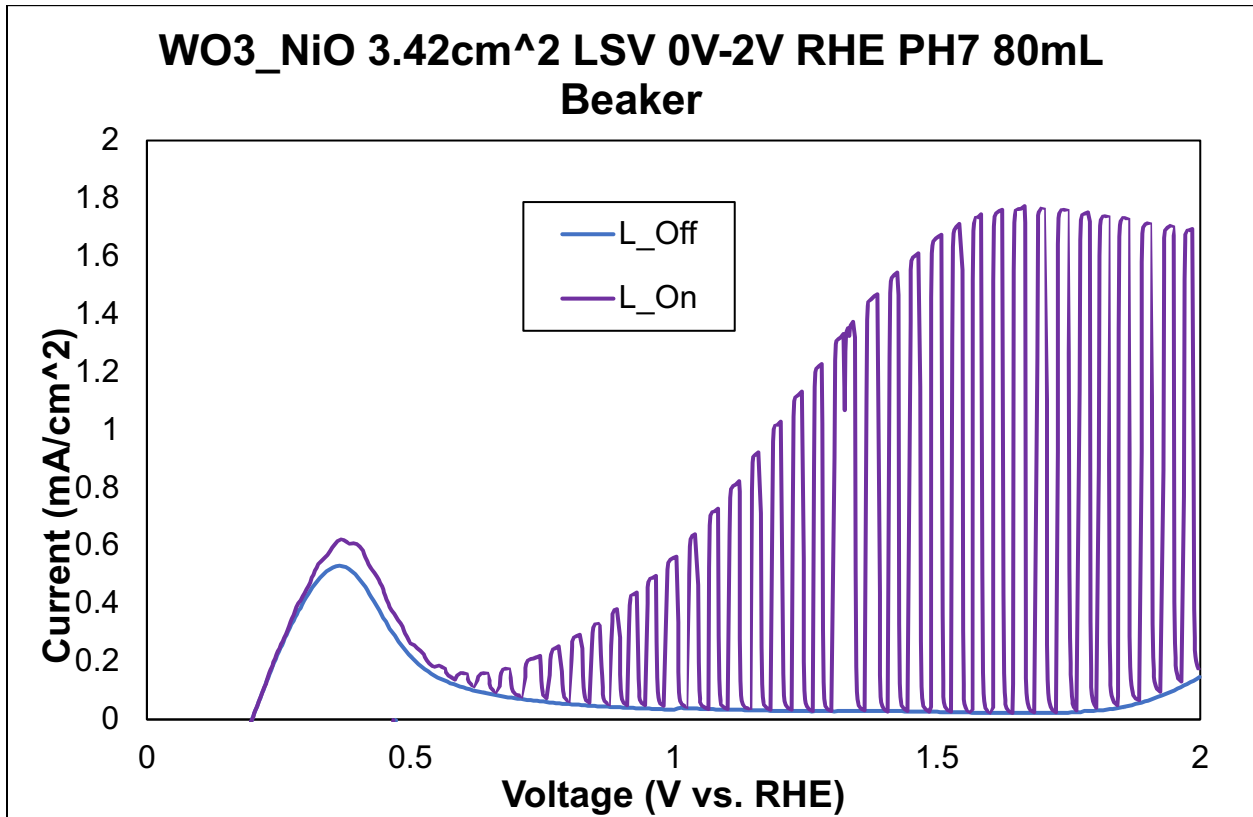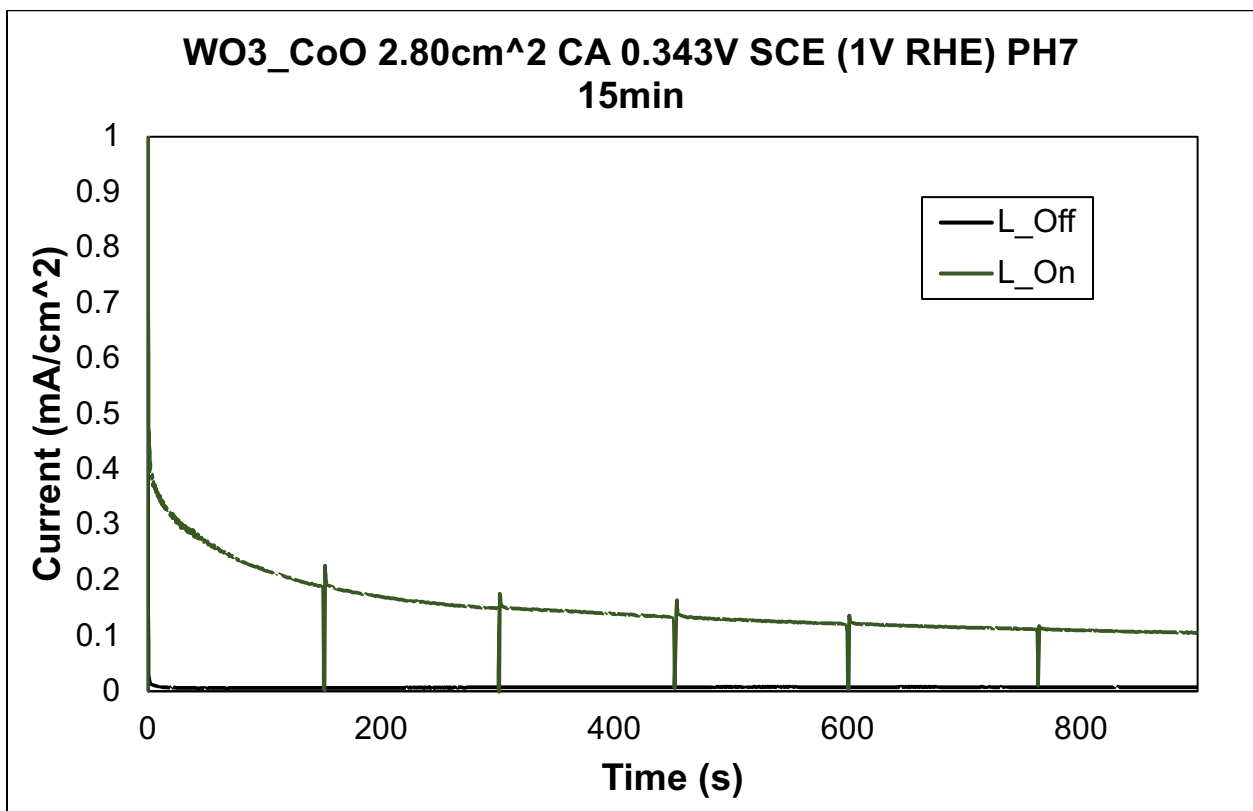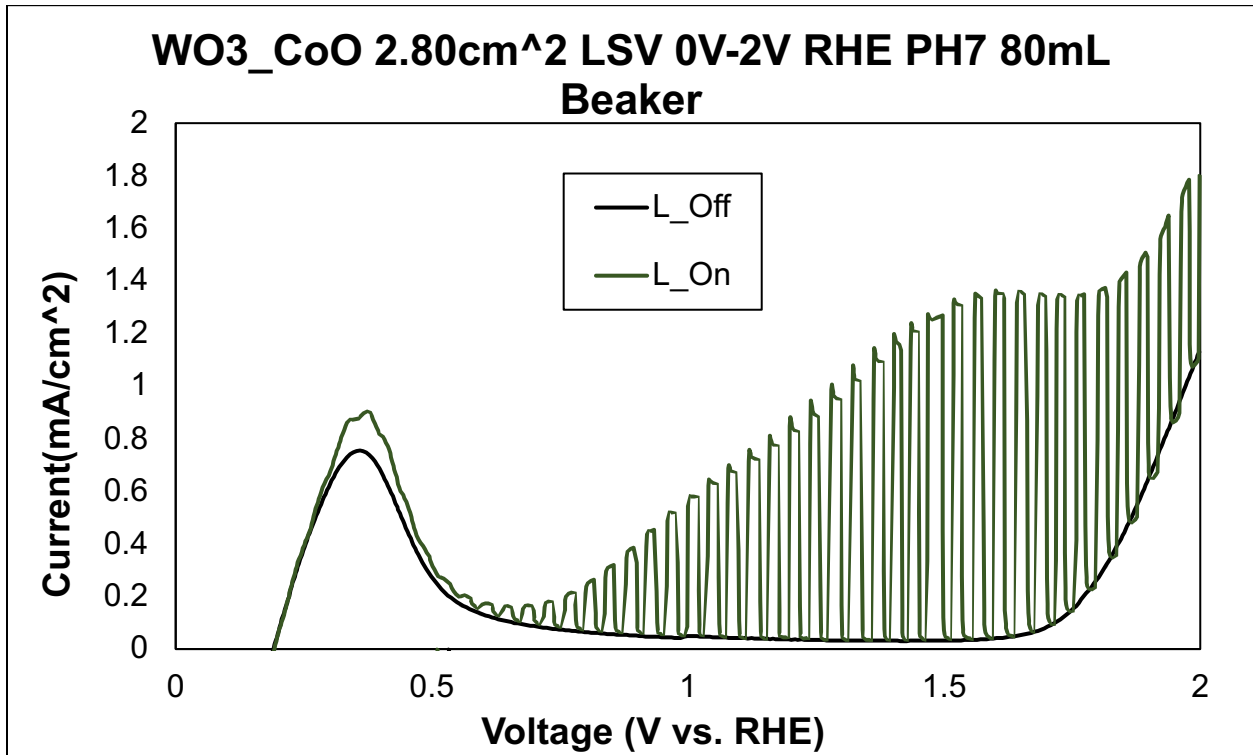
7.3. Appendix C: LSV/CA Plots

7.3.1 TiO2

TiO2 3.24cm^2 0V-2V RHE PH7 80mL Beaker

TiO2 3.24cm^2 CA 0.343V SCE (1V RHE) PH7 15min

WO3 2.52cm^2 LSV 0V-2V RHE PH7 80mL Beaker

WO3 2.55cm^2 CA 0.343V SCE (1V RHE) PH7 15min

WO3_NiO 3.42cm^2 LSV 0V-2V RHE PH7 80mL Beaker

WO3_NiO 2.80cm^2 CA 0.343V SCE (1V RHE) PH7 15min

WO3_CoO 2.80cm^2 LSV 0V-2V RHE PH7 80mL Beaker

WO3_CoO 2.80cm^2 CA 0.343V SCE (1V RHE) PH7 15min

SnO2_BiVO4 3cm^2 PH7 LSV 0V-2V RHE PH7 80mL Beaker

SnO2_BiVO4 3.15cm^2 CA 0.343V SCE (1V RHE) PH7 15min

SnO2_BiVO4_NiO 3.06cm^2 PH7 LSV 0V-2V RHE PH7 80mL Beaker

SnO2_BiVO4_NiO 3.06cm^2 CA 0.343V SCE (1V RHE) PH7 15min

SnO2_BiVO4_CoO 2.55cm^2 PH7 LSV 0V-2V RHE PH7 80mL Beaker

SnO2_BiVO4_CoO 2.55cm^2 CA 0.343V SCE (1V RHE) PH7 15min
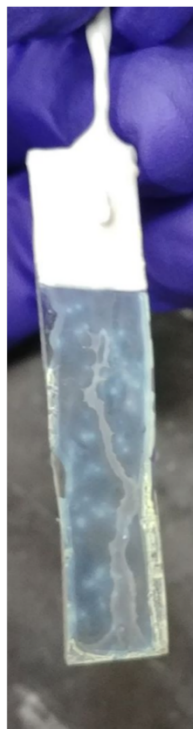
7.3.8 Summary of application methods

Table 1: Summary of different application test methods and their results.

#	Method	Conditions	Results
1	Original Spray Coating	4 Squirts (~50 mL) onto WO3 Cell @ 500C using hot plate, left for 1 hr	NiO did not seem to be produced. Left a yellow-like spotted pattern at the top of the cells. Temp Likely not hot enough
2	New Spray Coating	Glass preheated in oven set to 550 C. Glass removed from oven and placed on hot plate @ 550C. 1 spray (~13 mL) onto pre-heated glass, then placed back in oven for 1hr. (x2)	First layer seemed ok. Dispersion onto glass was splotched. Additional layers led to glass cracking when spray was used for coating. NiO seemed to be produced as no yellow coloring was left on the glass
3	Dip Coating	Completely submersed WO3 cell into NiO solutions (0.05, 0.1, & 0.2). Quickly pulled cell out of solution vertically, dried off back and bottom-most section, then layed horizontally. Set in oven at 550C for 1.5 hours	Layer was not completely dispersed onto the cell. Coating ran to the edges and clumped into circles in the middle of the cell.
4	Dip Coating + PEG	"" + add 2 g/ mL of PEG 3,000	"" - Layer burned? Completely black and smelled bad
5	Drop Coating	Dropped 300 (microL) onto top of the cell and transferred to oven @ 550 C (0.05 M)	Cell came back looking well. Evenly dispersed onto the cell and a thin film was left on the top of the cell. Black residue on top of cell..
6	Drop Coating + PEG	" + add 2 g/ mL of PEG 3,000	Cell completely burnt and coked.

7.3.9 Images to table 1 (7.3.8)
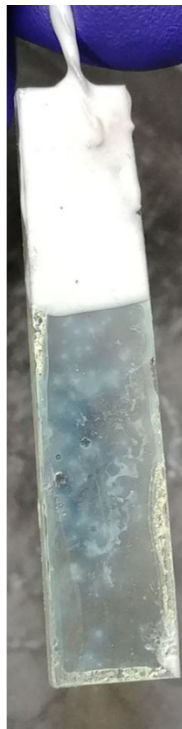
Dip Coating (3)   Spray Coating (2)   Spray Coating (2)   Spray Coating (2)   Drop-Coating (5)
                     (1-layer 0.05 M)   (2-layer 0.05 M)   (3-layer 0.05 M)   (Cell used for Natick)

Figure 47: Pictures to summarize the results of the different application methods of WO₃.